Fermilab

TM-1251
1620.000

SUPERCONDUCTING MAGNET TECHNOLOGY FOR ACCELERATORS*

R. Palmer
Brookhaven National Laboratory, Upton, New York 11973

and

A. V. Tollestrup
Fermi National Accelerator Laboratory, Batavia, Illinois 60510

March 1984

*Submitted for publication in Annual Reviews of Nuclear and Particle Science.

Contents

1 INTRODUCTION

A review article on superconducting magnets for accelerators should first answer the question, "Why superconductivity"? The answer revolves around two pivotal facts: (a) Fields in the range of 2 T to 10 T can be achieved; (b) the operating cost can be less than conventional magnets.

The relative importance of these two factors depend on the accelerator. In the case where an upgrade of an accelerator at an existing facility is planned, the ability to obtain fields higher than conventional magnets leads directly to an increase in machine energy for the given tunnel. In the case of a new facility, both factors must be balanced for the most economical machine. How to achieve this optimum is not yet clear.

In opting for superconducting magnets, one also takes on problems that have been foreign to accelerator technology until now. These can be lumped under these main headings: (a) Cryogenics, (b) quench protection, and (c) field quality.

At present, commercial refrigerators exist for large liquid He systems ($\sim$ 5000 ℓ/hr). At operating temperatures between $4^{o}K$ to $5^{o}K$, the ultimate Carnot efficiency is low, i.e., $\sim$ 1.4%, and the relative efficiency of a large plant ($\sim 10^{5}$ W at $4.2^{o}K$) may approach 30 percent. Thus, one needs 300-500 watts at room temperature for every watt of $4.2^{o}K$

load. This places strict requirements on the cryostat design, forcing one to use intermediate heat shields, super insulation, good insulating vacuum, and a minimum number of current leads between the cold conductor system and the outside world.

Other difficulties are imposed because of the cryogenic system. The continuity of the vacuum and cryogenic systems makes access to the beam difficult. Correction coils, pickup electrodes, etc. all require careful attention to details since the system must have a low heat leak in spite of many vacuum feedthroughs. Failure of even minor components means warming up an entire string of magnets which may take several days. The original installation relies on developing techniques to insure leak tightness of thousands of vacuum seals cooled to $4.2^{o}K$. This may sound difficult - it is! But techniques have been successfully developed to overcome these problems.

A second new regime of problems comes with "quench protection". A magnet quenches when some piece of the conductor is driven up in temperature until it loses its superconductivity, and at this point, the i^2r losses from the current in the conductor continue to increase the temperature. If the cooling is sufficient to overcome the heating, the conductor will cool and return to its superconducting state, the magnet is said to be cryostable. However, it is hard to achieve this degree of cooling in an

accelerator magnet where a very high current density is generally desired, although superconducting coils for bubble chambers are readily designed to be cryostable.

The temperature of the conductor may be driven up to the quench point by beam loss, frictional heat from the motion of the coil, or lack of sufficient refrigeration at coil support points. A successful design must protect every centimeter of conductor in a machine which may have several hundreds of kilometers of cable in the magnets. The problem is complicated by the inductance of the magnet which makes it difficult to reduce the current to zero in a short time. Quench protection complicates the design, but now known solutions exist.

Finally comes the question of field quality. An iron magnet has its field primarily controlled by the shape of the iron pole face. Laminations can be stamped to a precision and smoothness of better than .001 in. Classically magnet design has centered on shaping the iron correctly.

However, a superconducting magnet relies on accurate placement of the conductor to achieve the desired field. Conductors must be held in place to an accuracy of about .001 in. in order to achieve accelerator quality fields ($\delta B/B \sim 10^{-4}$). This is difficult because of the large magnetic forces and differential thermal stresses. A successful magnet will have a uniform field region for

between one-third and two-thirds of its available aperture. The space between the beam and the coil acts as a filter to remove the high harmonics introduced by individual wire strands and errors in their placement. Quality control of the components is required during the assembly, and a dedicated magnet measuring facility is the crucial final monitor of overall magnet quality. At the present level of technology, each magnet must be measured before installation.

Superconductivity was discovered by K. Onnes in 1911 and explained with a microscopic theory by Barden, Cooper, and Schrieffer in 1957. Type II superconductors using Nb_3Sn and NbTi have been developed since 1961. Thus, a long and difficult theoretical and experimental program lead up to the availability of conductor in the early 1970's that could be manufactured economically and could carry current densities high enough to be considered for use in accelerator magnets, and at this point, close collaboration between the conductor fabricator and the national laboratories resulted in the production of successful magnets.

The program above has culminated in the successful operation of the Tevatron early in 1983. The operational information to be obtained from this pioneering effort is crucial to the design of future accelerators. The basic magnet design used in the Tevatron has been reproduced at

DESY, Serpukov, Saclay, KEK, LBL, and BNL. Many variations and improvements are being investigated, and one can expect future machines, HERA and UNK, to have magnets with better quality and higher fields ($\sim$ 5 T). Such magnets were demonstrated at BNL for CBA.

Thus 75 years after the initial discovery of superconductivity, we can say that it has become a well engineered technology with a wealth of well understood solutions for the unique problems encountered. It is still difficult to predict beforehand if a particular variation of a magnet will "work". However, it can be stated that the sources of difficulties are well understood, and the necessary R&D program to produce a successful magnet is now well defined.

It is within this framework that we are approaching the greatest challenge - a superconducting collider in the 20 x 20 TeV range. It is here that the ultimate optimization between complexity, size, and cost will be made. We now turn to details of magnet technology.

2 MAGNET TECHNOLOGY

2.1 Coil Geometry

Magnets for accelerators require, in general, a vertical magnetic field in a long horizontal cylindrical volume. The coils of such magnets consist of long loops with conductor passing down one side of the magnet and returning up the other side. The magnet type can be

described by the typical cross section of such a magnet; the ends we will discuss later. We will divide magnets into three types. Low-field ion dominated magnets, high-field rectangular magnets, and high field magnets with circular cross sections.

For fields below 2 Tesla it is possible to design a magnet in which the field shape is dominated by the shape of magnetic poles above and below the field region. Such magnets are sometimes referred to as "superferric". Fig. 1 shows(1) an H magnet in which the conductor is relatively far from the field region, and the field is truly dominated by the shape of the magnetic poles. In this type, variation in position of the conductor will have essentially no effect on the magnetic fields. The poles have to be specifically shaped to obtain a good field in the central region and saturation, effects in these shaped poles usually limit the field to well below 2 Tesla. Fig. 1b shows(2) a superferric picture frame magnet in which the conductor is in the form of current sheets to the left and to the right of the field region. In this case no shaping of the poles is needed, and the entire space between the coils is, in principle, good field. The field is however to some extent dependent upon the conductor placement. The advantages are that less iron is required to return the field, and the design allows higher fields without large saturation effects. In neither of these cases is superconductor magnetization (persistant

superconducting currents) a problem. The superconductor becomes uniformly "magnetized" in a vertical direction, and the resulting field lines are returned in the iron without effecting the central field.

If fields significantly above 2 Tesla are required, then the iron in the poles of a magnet saturate and that part of the field above 2 Tesla has to be generated by the conductors themselves. Consider again the picture frame magnet as shown in Fig. 1b. As higher currents are passed in the two current sheets, the resulting field may be conceptualized as a uniform field from the iron plus a field generated by the coils alone. The field from the coils will not be uniform but will be higher at the left and right sides of the aperture and less in the center which is further from the conductors. In order to correct this non-uniformity of field, extra conductors have to be placed above and below the aperture as shown(3) in Fig. 1c. In this example, it is also seen that the aspect ratio of the coil has been changed to be relatively higher compared to its width in order to reduce the aforementioned non-uniformity of field. It is also seen that the cross section of conductor is greatly increased. In this example a field of 6 Tesla could easily be achieved with approximately 4 Tesla of that field generated directly by the coils, and approximately 2 Tesla contributed by the iron. The change of field shape as the field is incresed,

i.e. saturation effect, can be controlled by varying the relative current through the main coils and through the correction coils (sextupole correction coils) or self correction can be achieved by changing the pole shape from flat to an arch as is shown in Fig. 1c. This magnet, although conceptually based on the simple picture frame of Fig. 1b, is in now a hybrid between that picture frame designs and the circular designs which we will discuss next.

Since in high field magnets most of the field derives from the conductor placement, it is convenient to consider designs in which there is no iron present and all the field is so derived.

First we will consider a current sheet of uniform radial thickness surrounding a cylindrical field volume. The current density in this current sheet is arranged to vary as the cosine of the azimuth with maximum currents at the left and right, and zero currents at the top and bottom. It can be easily seen that such a current sheet will generate a uniform vertical field in the field volume. In practice the varying current density is approximated by a finite number of conductors and wedges (see Fig. 2a).

As an alternative, instead of varying current density in a current sheet of the uniform thickness as described above, one can keep current density constant and vary the radial thickness of the conductor. The resulting cross section illustrated in Fig. 2b is the space between two

intersecting ellipses. In practice this shape is approximated by one or more layers of conductor of fixed radial thickness as indicated in Fig. 2c. If three or more layers are used, a good approximation to the ideal field is generated. If only two layers are used, then the good field regions is restricted to only about 50% of the diameter within the coils. The field can be improved by the addition of wedges without conductor placed in both the inner and outer layers (see Fig. 2d). Since in the intersecting ellipse design the conductors are placed as close as possible to the field region, this design is both the most efficient in terms of conductor cross section for given fields, and also the one for which conductor placement is most critical. Magnetization effects at low field are also the greatest, and the design requires conductor of a keystone cross sectional shape which may be considered a complication compared to rectangular shapes. There is, of course, an arrangement (Fig. 2e) in which the intersecting ellipse cross section is approximated by rectangular conductors, and we see again the basic similarity to the picture frame concept.

2.2 Iron Cross Section

In the cosine theta design it can be shown that if the coil is surrounded by a concentric tube of iron and if this iron is placed at sufficient distance that no saturation occurs in that iron, then a strictly uniform field will

still be generated in the field volume. The point of maximum field in the iron is located at the inner circular boundary directly over the coil center. If this field is B_i, it can be shown that the field from the iron in the aperture is 0.5 B_i. Thus, if no saturation is allowed and B_i restricted to 2T, then the maximum additional field from the iron is $\sim$ 1 T (compare to the picture frame case where the iron may contribute $\sim$ 2 T). In intersecting ellipse designs, as in cosθ designs, the iron is usually in the form of a pipe around a coil cross section (see Fig. 1d and e). Although in this case, the coil cross sections have to be slightly modified in order to generate a pure dipole field.

The iron surrounding the coil can be either at the same temperature as the superconducting coil or at room temperature. In this latter case, space must be provided to thermally insulate the coil from the iron. This can be done in the case of Fig. 1a by keeping the field iron warm and providing insulation around the conductors. In the examples of Fig. 1b and c, it is not possible to have warm iron. For magnets illustrated by Fig. 2, either warm or cold iron is possible. If warm iron(4) is used, Fig. 1e, insulation is introduced between the coil package and the iron. In this case, the contribution to the magnetic field from the iron, because of its greater distance from the field region, is relatively less, and saturation effects may be avoided. If

the iron is cold(5a,5b), i.e. at the same temperature as the coils, then it may be brought in very close to the conductors (Fig. 1d) with a resultant increase in field, but with the disadvantage of increased saturation effects which have to be corrected by either correction coils or the use of crenalation(2) or holes suitably placed in the iron. Such holes are illustrated in Fig. 1f. A disadvantage of the use of cold iron is the large mass which must be cooled and the greater time and cooling capacity needed to perform this. Against this disadvantage must be weighed the higher fields achieved and the simplification resulting from the use of the iron both to retain the coils and to return the flux.

The radial thickness of iron required to return the flux can be approximately estimated assuming a saturation field of 2 Tesla in the iron. This thickness rises linearly with both the field aperture of the magnet and the magnetic field, while the mass rises almost as the square of these parameters. This mass can be reduced in the special case of magnets built for proton-proton colliding beam machines. For such machines, two magnetic apertures are required: one with the field up and the other with the field down. If these two apertures are placed side by side(6) in a common iron yoke, then field lines from one aperture are returned not through the midplane, but across to the other magnetic aperture. The total weight of iron in this (2-in-1 design)

is approximately the same for the double magnet as would be required for each of the single magnets (see Fig. 1f).

2.3 The Cryostat

In order to cool and maintain the superconductor at helium temperatures thermal insulation must be provided between it and the surrounding warm material. If the iron is warm, this thermal insulation must be provided in the relatively small space between the superconductor and the iron. However, in these designs the surface area which must be insulated is relatively small. In the cold iron designs space is not a problem, but the surface to be insulated is larger. In both cases in order to efficiently maintain the superconductor at helium temperatures, it is found desirable to introduce an intermediate shield, cooled either by liquid nitrogen or by returning the intermediate temperature helium gas.

For a two beam collider with coupled iron, only one cryostat is, of course, required for both beams with consequent savings. Even if uncoupled magnets are used, they can share a common cryostat.

Cooling to the conductor itself is usually provided by placing the conductor inside a helium filled cryostat with a flow of helium along the length of the magnet. In principle, and in simple test dewars, this helium is in the liquid phase at atmospheric pressure and heating causes the

liquid to boil and introduce a gaseous phase in the upper parts of the vessel. The danger that the presence of this gaseous phase will provide inadequate cooling to the upper coils has led designers to prefer single phase in the coil cryostat. This may be liquid helium at a somewhat elevated pressure or helium at a much higher pressure, above the critical point, in which case it is referred to as a super critical helium. In either case, the helium is caused to flow along the length of the magnet heat exchanging with the coil. The temperature of this helium will rise due to heat losses or heat generated in the coil until it is either replaced by new helium, Fig. 3a, or passes through a heat exchanger, Fig. 3c, exchanging heat with two phase helium. One attractive solution(7) used in the Tevatron, Fig. 3b, is to distribute such a heat exchanger along the outside of the magnet cryostat itself. Two phase helium in an annular space in contact with the cryostat flows in the opposite direction and heat exchanges with the single phase helium in contact with the coil. The temperature is held relatively constant, rising only as the pressure changes in the two phase return manifold.

Fig 3

Supports must be provided to hold the coils and other members that are at helium temperature with respect to the room temperature structures. These supports must be rigid enough to maintain the required positional accuracy but should have a low heat leak. The problem is complicated as

a little thought will show that ridigity and heat conduction tend to be proportional to each other for given materials.

In the case of a warm iron low field design as illustrated in Fig. 1a, no great positional accuracy is required, and little weight must be held, but little space is available to introduce long support rods. In a warm iron high field design the position tolerances are very tight, and again, there is little space for long support rods. One solution to the tolerance problem used in the Tevatron(8) is to supply supports which can be adjusted from the outside. The required positioning of the coil package with respect to the iron is then achieved after the magnet is operating by observing the field distributions.

In the case of cold iron designs, the weight to be supported is far greater than in the warm iron designs. However, there is adequate space to use relatively long support rods, thereby keeping the thermal losses low despite the larger cross sections required. Also the position accuracy required (at least in the case of the dipole bending magnets) is much lower in this cold iron case.

3 CONDUCTOR

At present the most widely used and commercially available superconductor is an alloy of Niobium (50 percent) and Titanium (50 percent), although Nb_3Sn was the first type II superconductor to be shown capable of carrying high current densities. Other alloys use components that are

prohibitively expensive, or they have undesirable mechanical properties that make the conductor or magnet fabrication difficult or impossible. In what follows, we will confine our attention to just NbTi and Nb_3Sn.

3.1 The B-J-T Surfaces

A superconductor behavior is specified by the current density, J; the magnetic field, B; and the temperature, T. In particular there is a critical current density for any B and T, beyond which the superconductor becomes normal. Such a three-dimensional surface for Nb_3Sn is shown in Fig. 4 and the projections on the J, B plane in Fig. 5a. Fig. 5b compares NbTi and Nb_3Sn at $4.2^{o}K$(9).

Fig 4

Fig 5

The maximum field at which superconductivity is exhibited is called the critical field. This is about 11 T for NbT_i and 20 T for Nb_3Sn at $4.2^{o}K$. Nb_3Sn shows its advantage in reaching fields greater than 10 T or in operating at termperatures higher than $4.2^{o}K$. However, it is brittle which leads to difficulties in magnet fabrication. NbTi is cheap, readily available, has good mechanical properties, and has now been extensively used for magnet construction (Tevatron, fusion reactor coils, and analysis magnets). Active development is in progress on both types of conductors, and one can expect, through careful control of the metallurgy, Nb_3Sn with better mechanical properties and NbTi conductors with still higher current density.

The design of a magnet is an iterative process. A coil design is chosen, and the current density in the coil required to reach a desired B_o is calculated. The field in the winding will be higher than B_o generally by 10 to 20 percent. One then checks the J, B graph to see if the operating point is inside the superconducting region by a safe margin (10-20 percent). If not the coil geometry is changed, and the calculation repeated until a satisfactory solution is found.

3.2 Stability

We must now consider the details of conductor fabrication, as it is much more complicated than discussed above for two reasons. The first concerns whether a conductor is in a stable state at a given B and I, and the second concerns whether or not the conductor destroys itself due to I^2R heating.

A simplified picture of current flow in a conductor was proposed by Bean and is useful to help understand the effects we will be discussing. Fig. 6a shows a very simple example of this model. A slab of type II superconductor with pinning is shown immersed in a magnet field $\vec{H} = \vec{e}_y H_o$. We assume the critical current is a constant, j_c, for a moment. As the field is increased, shielding currents start to flow in a manner that try to keep the field in the conductor equal to zero. However, the current density cannot be greater than j_c, and so the field penetrates a

Fig 6

depth such that $H_o = j_c\Delta$. As H_o increases, the field penetrates further into the sheet until $H_o = j_c a$. This is the maximum amount of shielding field the conductor can sustain. After this point, the field increase inside follows that of the outside field. Note that since flux is moving into a region, that there will be an Emf = $\partial\phi/\partial t$ which produces an E_z. This E_z combined with H_y gives $S_x = E_z H_y$, and energy flows into the conductor. A simple calculation shows that more flows into any region than is necessary to supply $W = \mu_o B^2/2$, the field energy, and the difference appears as heat, i.e., the moving field boundary is doing work against the pinning forces.

When the field is decreased, the same action takes place as above, except now the currents that flow are $\vec{J}_z = -\vec{e}_z j_c$, and the resulting field and current patterns are shown in Fig. 6b. Note that when the ouside field reads zero, that fields and magnetizing current still exist in the slab. The conductor is behaving very much like a piece of magnetized iron.

If now we consider the slab to be an idealization of a small piece of a conductor in a magnet, we can complete the picture. The field is the coherent effect of all of the current elements in the magnet, and the resulting shielding currents must be added to the transport curents to obtain the total current density. In general the coherent field is much larger than the local self field of current in a

conductor, and for this reason we can consider j_c to be approximately constant over the conductor. We shall see that the shielding field (i.e., the ΔB across a filament) is of the order of 0.1 T which is generally small compared to the field in the magnet.

We will next describe the fabrication of commercial superconducting cable and then use the model we have just described to understand why it has been necessary to develop such a complicated technology.

NbTi rods about 3 mm in diameter and 65 cm long are first fabricated. These rods are inserted into OHFC tubes with a round hole in the center and a hexagonal shape outside. The copper to superconductor ratio is determined by the outside dimensions of the copper hexagon and may vary from 1:1 to 2:1. The composite rods are stacked inside a 10 in. diameter copper shell and in vacuum a nose cone and base plate are welded on. This structure looking like an artillery shell is then heated and extruded in an enormous press (10^6 psi). The extruded conductor about 3 in. diameter is drawn through a succession of dies which reduces its diameter to final strand size, perhaps 1/2 to 1 mm. An electron microscope picture of a wire used in the Tevatron is shown in Fig. 7. Its end has been etched to remove the copper and reveal the filaments which are 10 μ in diameter; the o.d. is 0.6 mm. This incredible proces produces over 100 km of wire with 2,000

Fig 7

NbTi filaments encased in pure copper! Next 20 to 30 of these strands are made into a cable which can carry 5,000 A at 5 T.

Nb_3Sn is made with the same extrusion techniques. However, the alloy itself is very brittle and cannot be extruded. Hence, Nb and Sn are coextruded in various configurations. After the cable is fabricated, it must be heated to $\sim 700^{o}C$ for a number of hours, which allows the Sn to migrate into the Nb and form the superconducting alloy. After this treatment the cable may not be bent to radii less than about 5 cm without loss of capacity. Sometimes, therefore, the reaction is performed after the coil is wound. This is a difficult fabrication technique as the dimensions of the coil change during the heat treatment. Subsequently, it must be handled very carefully during magnet assembly, and insulation has to be impregnated into the coil in its wound form.

The small filaments are necessary for several reasons. The first is called the adiabatic stability criterion and arises from the following reasoning. Flux penetrates a type II superconductor as we explained using the simplified model due to Bean. The current density at each point is given by the critical current, $j_c(H)$, for the local field. If the temperature in the filament should rise δT_i for some reason, the value of the critical current will decrease, and the field in the filament must penetrate deeper. This change in

the field causes a local deposition of heat in the filament which will remain in the NbTi because the diffusion times for heat are much longer than the characteristic times for changes of field. This heat raises the temperature of the conductor by δT_f and if $\delta T_i/T_f > 1$, a runaway condition will exist. Since the magnetic energy stored in a filament is a function of its size, one can calculate that for stability:

$$J_c^2 d^2 < -\frac{3}{\mu_o} (C_p \rho) J_c/(\partial J_c/\partial T)$$

where C_p is the heat capacity, ρ the density, and $\partial J_c/\partial T$ the change in critical current with temperature. $J_c(\partial J_c/\partial T)^{-1}$ is $5^{\circ}K$, and $C_p\rho$ is $\sim 10^{-3}$ Joules/cm^3. Substituting in the above equation gives $d < 30\ \mu$.

So the first reason for the copper matrix is for mechanical support of the fine filments. It also aids in transporting away any heat generated in the filament as its heat conductivity is almost 3 orders of magnitude greater than the superconductor.

The second reason the copper is necessary is to protect the magnet if the conductor should be driven normal. The resistivity of the superconducting filament once it goes normal is so high that it essentially transfers all of the current to the copper. The copper carries the current until either the He reduces the temperature to less than T_c or until the magnet is de-energized. If the cooling is greater than the I^2R heating, the conductor will recover its

superconducting state, and the magnet is said to be cryogenically stable. Bubble chamber magnets are in this category because their stored energy is so large that it would be impractical to remove it in a short time. Accelerator magnets require such a high current density that space for copper and He in order to achieve cryogenic stability is not available. Hence, these magnets must have either an active or passive quench protection systems.

In the case of Nb_3Sn conductor, copper is also introduced between the filaments to separate and support them, but in the course of the reaction with the tin, the copper is converted into bronze whose resistance is too high to provide the needed stability. Therefore, a barier layer is introduced, and a region of pure copper is maintained outside this barrier.

3.3 Hysteresis and Eddy Currents

A magnet with 100 turns of 23 strand cable has several million filaments carrying the magnet current. A filament in a uniform field will have an induced dipole moment due to the shielding currents. These dipoles act coherently much the same way as the atomic current in a piece of iron - i.e., there is a magnetization dipole moment per unit volume. This magnetization effect in a pulsed magnet causes the actual field to lag the field produced by the transport currents and in accelerator magnets shows up in the dipole and sextupole terms of the field expansion. The magnitude

of these magnetized fields can be as large as .001 T, and they are important in determining the field shape. The effect is proportional to filament diameter.

These same currents as indicated earlier also result in an energy loss when a magnet is pulsed in a cyclical manner. Since the B-H curve is open, energy is deposited in the magnet each cycle and is proportional to the filament diameter for a fixed coil geometry and is also roughly proportional to B_{max}.

A second source of perturbing fields and ac losses is from the eddy currents in the cable structure. Consider the following simple picture. Flux threads a loop of resistance R and area A. If B rises linearly from 0 to B_o in time T_o and back to zero in the same time, we can calculate the energy dissipated in heat.

$$\frac{W}{\text{cycle}} = \left(\frac{B_o}{T_o} A\right)^2 \frac{1}{R} 2T_o = 2\, B_o \dot{B}_o A^2/R$$

In this equation, the term in parenthesis is the induced Emf which generates a constant power for a time $2\, T_o$. The equation shows that the losses are proportional to B_o and $\dot{B}_o$. We saw that the hysteresis losses were proportional to B_o so we can write an expression the total loss/cycle of a linearly ramped magnet

$$W/\text{cycle} \sim \underbrace{K_1 B_o}_{\text{hysteresis}} + \underbrace{K_2 B_o \dot{B}_o}_{\text{eddy current}}$$

These losses may be separated by ramping the magnet to different B_o with different $\dot{B}_o$. For the Tevatron(10) the hysteresis loss is about 200 J/cycle when the magnets are ramped to 4 T. (These magnets are 6 m long with a bore of 7.5 cm). The eddy current loss is negligible. However, some of the very early models that were constructed with a cable that was filled with solder had eddy current losses of > 1 kJ/cycle.

There is a phenomenon closely related to eddy currents that can effect the performance of a magnet. We pose the question: How does one know that all of the strands in a cable are carrying the same current and even more detailed, how does one know the filaments in a strand are equal participants? Current sharing is governed as follows: Consider two strands through a magnet. They are connected together at each end and along their length by resistive contact between strands in the cable. During ramping, the strands can be represented as two inductively coupled loops. To equalize the currents, it is important that there be no net flux from the main field that links the area between the two strands. If this is the case, the net inductance of the loop comprising the two strands will be very low, and the contact resistance, or resistance of the matrix will allow equalization of any small current differences that may exist.

The decoupling of strands is accomplished by either braiding the strands in the cable as was done for ISABELLE or spiraling the strands in a cable as in the Fermilab-Rutherford cables. In addition, when the cable is fabricated, each strand is given a twist about its own axis every inch or so to decouple the individual filaments. The cable is a much more complicated structure than casual examinatio [illegible]scloses!

One may ask why not insulate the individual strands in the cable? However, this leads to very erratic magnet performance which has been traced to unequal strand currents since it is difficult to decouple completely the interstrand circuits from the main field. On the other hand, good contact between strands leads to high eddy current losses and a magnet whose field shape is dependent on B. The Fermilab-Rutherford cable has solved this problem by coating every other strand with CuO, which has enough resistance to control the losses without being so high that current sharing is upset.

3.4 Temperature Effects

It has been mentioned previously that Nb_3Sn has a higher critical field than NbTi. However, the critical field for NbTi can be increased by decreasing the temperature. Fig. 5b compares the two conductors at different temperatures. The interesting prospect arising here is to investigate the behavior of a conductor below

2.17°K, the λ-point for HeII. Large accelerator type magnets have been successfully operated at 1.8°K, with the expected increase in field due to the higher J_c. The superfluid properties of HeII show remarkable effects on the magnet stability, presumably due to the improved cooling from the superfluid. This approach is being studied extensively at LBL(11).

A question that remains to be answered is whether the decreased Carnot efficiency at the lower temperature will be a practical limitation. At present at 4.2°K, the overall efficiency is about 400 W/W at 4.2°, i.e. large refrigeration plants only have an overall efficiency of about 15 percent of Carnot. It may be that a point favoring Nb_3Sn is that even at present fields it can operate at higher temperature with resulting higher efficiency and lower operating costs for the refrigerator.

4 FIELD QUALITY CONSIDERATIONS

4.1 Field Analysis

In the central part of a long magnet the fields have no axial components. It is conventional to express the distribution of transverse magnetic fields on the horizontal midplane as a quadratic expansion of the distance from the magnet center. The fields at any point (r,θ) in the vertical direction (B_y) and horizontal direction (B_x) are then given by:

$$B_y = B_o \{1 + \sum_{n=1}^{\infty} \left(\frac{r}{r_o}\right)^n (b_n \cos n\theta - a_n \sin n\theta)\}$$

$$B_x = B_o a_o + \sum_{n=1}^{\infty} \left(\frac{r}{r_o}\right)^n (a_n \cos n\theta + b_n \sin n\theta)$$

r_o is a reference radius usually taken at a given fraction (2/3) of the coil inside radius.

The radial and tangential components of these fields have a periodic variation in the azimuthal angle θ where the number of poles $m = 2n + 2$. They thus represent various multipole components of the field. The coefficient of these multipoles a_n and b_n are determined by the current density distribution. If the current density in a shell can be written as being proportional to $K_n^{(e)} \cos n\phi + K_n^{(o)} \sin n\phi$, then $a_n \sim K_{n+1}^{o}$ and $b_n \sim K_{n+1}^{(e)}$. Thus, the symmetry of the current distribution is reflected in the a_n, b_n. A coil that is symmetrical both up and down and right and left has only even b_n. It helps to visualize these fields if one notes the absolute value of field for a given multipole, $|B_n|$, is constant on any circle about the origin, and that this vector rotates n+1 times during a traversal of such a circle. Its magnitude is $\sim r^n$.

The use of such a multipole formulation has various advantages. Many specific behaviors of the accelerator are related to specific multipole components. The dipole (B_o), for instance, determines the equilibrium orbit of particles, and the quadrupole moment (b_1) effects the focusing of the

beam. The sextupole provides momentum dependent focusing and so on. A second advantage of this formulation is that it allows an easy estimation of the effect of different field errors as a function of the radial size of the beam. It is also convenient to design correction coils which have explicit multipole contributions which can be used to correct unwanted components present in the main magnets.

The situation at the end of a magnet is more complicated, the conductors make the turn from passing up one side of the magnet to pass down the other side. The multipoles tend to vary rapidly in this region, and the magnetic fields contain axial field components. However, the effect on the beam is dependent primarily on the integral of the transverse fields and is very little affected by these axial field or the details of variations of the transverse fields. The end contributions to these integrals can be obtained by calculating or measuring the multipole integrals for the entire magnet and subtracting the multipole contributions from the central part of the magnet multiplied by some suitably chosen effective magnet length.

4.2 Field Precision Requirements

The field requirements depend, of course, on the details of the machine in which they are to be used and on the beam size stored in that lattice. Field requirements thus cannot be specified without knowing these details.

Nevertheless, it is convenient to give at least order of magnitude values that have been found to be required. If sufficient correction elements are included in the design, variations in the dipole field components may be allowed to vary about one part in 10^3. Quadrupole and sextupole components over a defined good field region should be within 2×10^{-4}. For higher multipoles, correction is clearly not possible and allowed errors should be less than 10^{-4}. In some cases as for a stacking ring, the "good field region" may extend over as much as two-thirds of the coil inside diameter. In other cases if injection, for instance, is at a high energy and the beam is already small, the required good field region may be one-third, or even less, of the coil inside diameter.

When a magnet is energized some changes are observed in measured multipoles. In practice these changes are very small in the so-called unallowed multipoles, namely, all the multipoles except in the even b_n terms. Several effects can, however, generate changes in the even b_n terms. Magnetic forces will cause small motion of the conductors and cause changes in these multipoles. Changes in multipoles can occur due to persistent currents and saturation. These effects will be discussed below, but they are not a problem providing they are the same for all magnets.

4.3 Coil and Iron Cross Section Design

In the case of a simple picture frame magnet as illustrated in Fig. 1b, a uniform field is achieved from the intrinsic design. In all other cases the iron or coil shapes must be designed specifically to achieve the uniform field. If good field is only required over say one-third of the aperture, then very simple approximations to the correct iron or coil shapes may be used (Fig. 2c for example). If good field is required over as much as two-thirds of the coil inside diameter, then more complicated approximations (such as Fig. 2d) must be used.

In order to get an understanding of the effects of errors of coil placement on the magnetic fields, we examine the multipoles that would be generated by random displacements of coil blocks in a particular case. The calculations were performed for a design of the type represented by Fig. 2a but are applicable for any circular magnet. In each case the coil is divided into 24 (6 per quadrant) equal parts, and each part is allowed to have a random displacement in two directions of 10^{-3} times the coil inside radius.

Table I shows the resulting calculated variations of the various multipoles together with the measured(7) variations in a set 10 otherwise CBA magnets whose coil inside diameter was 6.6 cm (i.e. the random motions in this case were 66 μ). The table also shows the ratio of observed to calculated variation.

It is seen that the ratios of observed to calculated errors are systematically higher for even b_n and odd a_n terms, compared with odd b_n and even a_n's. These systematic effects indicate that block placement errors are correlated. It is instructive to study cases of particular coil errors that will generate particular lower multipoles. In Table II we give the magnitude of the induced lowest multipole corresponding to a particular set of 10^{-3} errors. We also give the magnitude of such errors that would produce the observed variations given in Table I.

The particular cases given are:

a. A 1 milliradian horizontal shift of both pole spacers. This causes a compression of all coils on one side and an expansion of those on the other. Such an error introduces a left right asymmetry and generates only odd b_n terms. In the example such errors were not greater than 14 μ rms.

b. A vertical displacement of the horizontal midplane. The coils in the upper half are uniformly smaller and those in the lower half uniformly larger. This gives a pure up down asymmetry and induces only odd a terms. This is seen to be a more serious type of error; in the example it is of the order of 40 μ rms.

c. An asymmetric vertical displacement of the horizontal midplane: higher on one side, lower on the other. Such an error would arise if there were left right asymmetries in the coil curing fixtures. In the example this error is not greater than 16 μ rms.

d. In this case the conductors are assumed to have current density varying uniformly from the midplane to the pole in such a way as to produce a maximum azimuthal displacement of 10^{-3} radians half way up the coil (the displacement always being towards the midplane). Such an effect is produced by variations in the friction either during cure or assembly of a coil. It is a four-fold symmetric effect and can only induce even b terms. In the example this is a relatively large effect: 34μ. We must note, however, that variation in persistent currents or iron saturation could also cause fluctuation in this term.

e. The coils are assumed to be located on a radius larger or smaller than designed, the error being one part in 10^3. The primary effect is to vary the central field (B_0). The observed variation in the example indicate radial errors somewhat less than 10^{-3}, corresponding to 45 μ, but it must be remembered that b_0 variation can also come from magnet length and other errors.

These observations suggest that the required field accuracy is not severly limited by the position of the poles or the radial dimensions, but is dominated by errors in coil size and conductor uniformity. Since such errors will scale down in a smaller magnet, we may hope that the multipole fluctuations arising from them will also scale, i.e., the even b's and odd a's will not greatly increase in a smaller magnet. The odd b_n's and even a_n's which may already be dominated by pole position errors would be expected to rise in inverse proportion to the coil size.

We will now discuss the precautions taken in the construction of these magnets which were needed in order to achieve these high accuracies.

Firstly, it is necessary to control the dimensions of all the components which support the external dimensions of the coils. The iron laminations must be accurately punched, the pole spacers must be accurate as must all the insulating materials on the outside and at the poles of the coils. All these dimensions can be held to approximately 25 microns. The conductor wire insulation and epoxy glass covering must also be controlled as well as possible. However, even when these dimensions are held to 5 microns per turn, the accumulated error in a coil stack of 60 turns is as large as 300 microns and clearly unacceptable. In order, therefore, to control the dimension of a final stack, the following

procedure can be followed. The coils are first cured at a pressure such as to give dimensions sightly larger than those finally required. The coils are then measured at their final precompression and using this data the coils are recured to a final dimension chosen to produce coils of the correct size. A second measurement at final precompression is used to check that the size within 25 microns or a second recuring can be undertaken to correct any deviation. The coils are finally assembled between the yoke supports with teflon slip planes placed between the coils and their support and between the two coils to keep friction low.

A somewhat different philosophy was adopted for the Tevatron magnets. In this case great emphasis was placed upon constructing a factory that would produce a very uniform product, but absolute coil shape was given secondary importance. If one assumes for the moment that there are no random errors, then systematic errors can be corrected by means of small shims placed in the coil in such a way that they cancel the undesired moments. These shims are calculated on the basis of magnetic measurements made on the production stream flowing from the factory. This closes a feedback loop around the factory which can correct for any slowly changing systematic errors in the production stream. For this method to work, random errors must be constrained by good quality control, and the delay between production and measurement must be kept small. Nearly 800 dipole

magnets and over 200 quadrupole magnets have been measured for the Tevatron. The characteristics of these magnets are in the literature(113a,13b).

4.4 The Magnet Ends

If the magnet ends are designed with engineering considerations in mind and no special care is taken, then it is likely that significant multipoles will be contributed by these end regions. Such multipoles can be corrected in an integral sense by slight modification in the design of the central part of the magnet. Since the magnet is straight and since the beam bends, this correction is not simple. It may be desirable to design ends that contribute no unwanted multipoles. As an example, we consider a very simple $\cos\theta$ design as illustrated by Fig. 8a, which shows a z plot of the end of the conductors, i.e. what the conductors would look like if they were unwrapped from the beam pipe and laid out onto a flat surface. A section (yy) through the end shows that the conductors are now concentrated nearer to the poles yielding relatively higher fields in those regions, and relatively lower fields at the midplane. Such a field has a strong negative sextupole component. The addition of spacers within the end windings as illustrated in Fig. 8b can correct these multipole components.

Fig 8

The accuracy requirements in the location of the conductors at a magnet end are less stringent than those for the placement in the center of the magnet because of the smaller contribution to the total magnetic field given by the ends, and no problems in such accuracy is usually experienced.

4.5 Superconducting Persistent Currents

Eddy currents in a superconductor have, of course, an infinite time constant and produce an anti-ferrimagnetic magnetization behavior. When the magnet is first excited these currents are developed and rapidly increase until they reach the critical current within the superconductor. They then become damped by the onset of resistivity in the superconductor and become futher damped as the field rises and the superconducting critical current falls. When the field in the magnet is reduced, eddy currents will be generated in the opposite direction and will again follow a bound set by the critical current behavior of the conductor.

As it has been stated above, in a simple picture frame magnet these magnetization effects do not produce changes in the fields in the good field region. However, in other geometry designs they do perturb the good field. Fig. 9a shows the effects on the sextupole component (b_2) in a magnet in which the iron is relativelv far from the coil so that there are negligible saturation effects. The lower line indicates the sextupole component observed while the

Fig 9

current was rising and the upper line that observed while the current was falling. The difference between the two lines indicates a contribution from the magnetization. Such effects are corrected by trim coils and present no problems in principle. However, variations in the superconducting material in the cables can produce variations in these magnetization effects magnet to magnet and correction of these effects is more difficult. Variations in niobium-titanium cable are probably of the order of 5% (although there is some evidence(8) that the true fluctuations are significantly less), and it is thus necessary to keep the magnetization contribution to less than 20 times the precision requirements specified above. The effect when expressed as a ratio to the central field is, of course, far worse as the central field reduces since not only the denominator decreases, but magnetization effects in the conductor increase roughly in inverse proportions to the field due to the increase of j_c. The effect is worse for a higher field magnet since more superconductor or better superconductor is employed. In practice these two effects result in a dependency on the ratio of injection and final field, little dependent on the absolute fields. It is worse for smaller aperture magnets where the good field region is closer to the conductor. It can be reduced by reducing the individual filaments within the superconducting cable (see Section 3). The effect can

be expressed:

$$\frac{\Delta B_1}{B_1} = \text{const}\ \frac{F_1}{F_2}\left(\frac{B_2}{B_1}\right)^2 \frac{\mu}{r} \approx \text{const}\left(\frac{B_2}{B_1}\right)^{1.5}$$

where F is the pinning force of the conductor, i.e. the product of the critical current times the local magnetic field, B_2 is the field of the magnet, μ the filament diameter, and r the coil i.d., the subscripts refer to the injection (1) and final fields (2). The constants depend on the geometry of the coil used.

4.6 Iron Effects

Below 2 Tesla variations in iron permeability (μ) and coercivity will dominate the field of a magnet. Iron can be obtained(9) with specified variations of $1/(\mu-1)$ of $\cdot 2\ 10^{-4}$ rms. The effect of this on the central field is typically multiplied by a factor of 5 yielding central field fluctuations of the order of 1×10^{-4}. The coercive force can be specified to within ±0.2 Oersted rms and generates typically central field changes of ±.6 Gauss thus producing field errors of only $1.5\ 10^{-4}$ at a typical injection field of 4000 Gauss.

At fields above 2 Tesla and if the iron yoke is relatively close to the coils such that the fields in the iron significantly exceed 2 Tesla, then saturation effects in the iron will produce a reduction in the transfer junction (the ratio of central field to coil current, see Fig. 9c). The effect is due to the sharp reduction of μ at

high fields which is given approximately by

$$\frac{1}{\mu-1} = a + \frac{H}{M_s}$$

where a is a constant, H is the field in the iron, and M_s the saturation induction. In a CBA magnet at 6 Tesla the dependence of the central field (B_0) on the iron saturation induction (M_s) was:

$$\frac{\Delta B_o}{B_o} \approx \frac{1}{4} \frac{\Delta M_s}{M_s}$$

The observed rms variation in M_s was 0.13% which produced central field variations of $3.3\ 10^{-4}$.

Saturation will also in general produce significant changes in the multipole content within a magnet. If, for instance, we look at the sextupole component b_2 for a magnet with the iron close to the coil as is shown in Fig. 9b, and if we compare this with Fig. 9a, then we observe changes in the sextupole moment above 2 Tesla fields which arise from these saturation effects. This high field magnetization can be qualitatively understood as an initial rise in the sextupole moment due to saturation of the iron in the immediate vicinity of the pole, followed by an eventual fall in the sextupole component which is caused by effects from the saturation of the iron in the magnetic return on either side of the coil package. A balancing of these two effects at the maximum field can be used to reduce the strength of correction coils required. Like the magnetization effects

these saturation effects are not intrinsically a problem providing they are the same for all magnets. The oserved magnitude of fluctuations in these effects was 1.2 10^{-4} at 2/3 aperture.

Saturation effects can be reduced by shaping of the magnetic pole, by crenelation, or by the introduction of holes within the body of the yoke. An interesting example of the use of holes is provided in the case of the design of 2-in-1 magnets. In these magnets saturation effects occur not only in the even harmonics of beam, but also in the odd harmonics, since left right symmetry is not maintained. In particular, a quadrupole moment is induced which while it can be corrected requires additional coils. With the introduction of a hole placed between the two coils as had been indicated in Fig 1f all significant quadrupole saturation effects can be eliminated.

4.7 Correction Coils

In almost any accelerator correction coils will be required, correction dipoles will be used to control the central orbit of the machine, correction quadrupoles will be employed to adjust the tune, and sextupoles will be used to control the chromaticity, that is, the variation of tune with momentum. If all magnets were identical, these correction coils could be the same at all points around the ring. However, in order to correct for errors both in surveying and in the magnet it is usually necessary to

provide at least the dipole correctors with separate power supplies for each correction coil. A more limited number of power suplies are usually used for the quadrupole and sextupole correctors. The current in these correction coils must be adjusted as the main field in the machine is increased so as to correct the persistent current saturation, coil motion effects, and saturation effects. Since the persistent current and some magnetization effects at low field are dependent on the previous history of the magnetic fields, it is necessary to cycle the machine in a prescribed manner and to determine the correction currents required for this particular cycle. It should be also noted that in the case of persistent currents, their effects are strongly dependent on the temperature of the superconductor and thus good control of this temperature is required if more complicated corrections are to be avoided.

Ideally a correction coil to correct a defect in a particular magnet such as saturation or magnetization should be located at its source, i.e., it should be located within the magnet itself. In the case of large bore magnets where there is no shortage of space between the coils and the beam tube--this can be done. Coils with different multipole moments can be wound in layers on the bore tube and such coils can be designed to show little training and near full short sample current carrying capacity.

An alternative to placing the trim coils within the magnets themselves is to wind special short trim magnets and place them relatively more sparse position around the ring. This while not theoretically so ideal is almost certainly a more economical course even though slightly a larger proportions of the machine azimuth must be devoted to this purpose. Such a solution is used in the Tevatron(16a,16b).

5 FORCES AND COIL PACKAGING

A conductor in a field of 5 T and carrying 5,000 A experiences a magnet force of 25 kg/cm. Such currents and fields are typical in the magnets we are discussing. Since a magnet may have 100 such conductors in its cross section, it is immediately evident that the total forces which must be contained by the support structures are enormous. Containment of these forces is complicated by the fact that the structure is at 4.2°K and must have a limited heat leak to the outside environment. In addition, the quality of the field is determined by the accuracy of the conductor placement and, consequently, the support must be very rigid so that the conductors do not move as the magnetic field changes. Finally, the large thermal contractions of the different components must track each other in order for the package to be mechanically stable when cold. To appreciate the magnitude of this latter problem, we remark that the coil package for the Tevatron magnets shrinks 3/4 in. axially when cold, and the diameter changes by .020 in.

5.1 Magnet Forces

Let's start by considering the magnetic forces. The simplest picture has a field with a magnetic presure, $B^2/2\mu_o$, which is equal to 100 kg/cm^2 for 5 T. This force tries to blow the magnet apart both longitudinally and transversely. In the axial direction, the magnet is held together by the conductor itself. Transversely the forces must be absorbed in a cold rigid structure called collars or yoke. If one examines F = j x B in cylindrical coordinates, one finds both an azimuthal and radial component for the force. The azimuthal force compresses the coil package, and Fig. 10 shows these two components for the conductors in the two shells of the winding for the Tevatron magnets.

The collars must be strong enough to resist the sum of the radial forces without deflecting more than a few mils. Small elastic deflections lead in first order to a sextupole moment that is a function of I^2 and may be compensated by dynamic correction coils (which are required for many reasons). For a pulsed machine, a more important consideration than deflection of the collars is their fracture by fatigue(17). This limits the maximum stress to less than about 30 percent of the yield point. Magnets with cold iron (ISABELLE), of course, don't face this trouble as the support is massive and in storage rings the number of cycles during the life of the machine is not large.

We now consider azimuthal forces. Note that the largest forces occur in the turns nearest the poles decreasing to zero at the midplane. In a two-shell magnet, these forces are largest for the inner shell. Since there is no constraint on the winding in the azimuthal direction (i.e., winding can slip relative to the collar surface), the forces of the wires sum as one approaches the equator. The top half of the coil balances the bottom half. In the Tevatron, the azimuthal forces sum at the midplane to 250 kg/cm in a direction to compress the coil. If the elastic constants of the top and bottom half of the coil are the same, there will be no motion of the midpoint, but there is an elastic compression at $\sim\pm 30^{\circ}$ toward the midplane which induces a sextupole moment. If the elastic constants are not equal, the midplane can move, and quadrupole moments will result.

5.2 Preload

We are now in a position to discuss a difficult problem in magnet construction. If the azimuthal forces of the last section were allowed to act on a coil which is only supported in the radial direction, the coil will compress itself as it is excited and the angles of the shell will change. If these change symmetrically, a sextupole moment will be induced and if asymmetrically, quadrupole terms as well will appear. The field is enormously sensitive to these angles - they must be maintained to an accuracy

of ~25μr for adequate field quality. The forces are so large that with the elastic modulus available in the insulated coil packages ($E = 10^6$ psi), the compression of the coil would far exceed this limit. As a result, when the coil is constructed, it is preloaded in the azimuthal direction to the extent that the elastic forces are greater than the magnetic forces. This ensures that the boundaries of the coil package will stay in contact with the collars during excitation. The Tevatron coils(18) were assembled in a large press, and the CBA magnets were bolted together with a similar pressure. Elastic motion of the coil relative to its support can still take place but at a much reduced level. (It is similar to fixing two ends of a loaded beam, compared to fixing only one end.) Elastic motion can also be reduced by making the elastic modulus high. The group at LBL has had successes in achieving $E \sim 4 \times 10^6$ psi which is perhaps four times larger than achieved in the Tevatron magnet; the CBA coils had 2×10^6 psi.

The problem of adequate preload is greatly complicated by the fact that when the temperature is reduced all the components become smaller. Stainless steel has a fractional change of 3×10^{-3}. The coil package is much larger and also less reproducible or predictable because it is a composite of superconductor, copper, and insulation in a configuration that must be porous to allow He penetration. As a consequence, the preload established at room temperature is

reduced as the temperature is lowered. Careful measurements of this effect must be made and compensated for at assembly time. If the contraction is α, the modulus E, then the total pressure at room temperature is $p_o = \alpha E + p_M$, where p_M is the magnetic pressure. Shorts may develop if p_o is so high that the insulation is crushed. Successful packaging must involve an elaborate development and test program where the designer is empirically feeling his way through a maze of unfriendly materials problems. Our discussion above has assumed the elastic modulus is linear, which it is not! As the operating fields increase, the preload must increase, and new higher strength coil packages must be developed.

6 QUENCH: THEORY AND MAGNET PROTECTION

A magnet is said to quench when some portion of the conductor goes normal for whatever reason, and the ensuing I^2R heat is greater than the cooling so that still more of the conductor is driven normal. Accelerator magnets require very high current densities to achieve fields of 4-5 T in the bore, and there is never enough cooling to return the conductor to its normal state. For instance, in the Tevatron magnets which carry 4,000 amps, if the cable goes normal, the I^2R heating is 16 watts/cm of cable, whereas the cooling by the He is at most a few tenths of a watt. Thus, the area spreads. The velocity along the cable is 1-10 m/sec but due to the insulation and He between turns, the time to jump to adjacent turns is milliseconds. As will be

discussed later, the current must be rapidly reduced to zero ($\sim$ 1 second) or the conductor will destroy itself at the point the quench started since that is the hottest spot in the magnet. We start by describing various quench mechanisms.

6.1 Quench Theory

Fig. 11 is an attempt to elucidate the energy diagram of an excited magnet. The curve is the enthalpy of 1 cm of 23 strand Tevatron cable as a function of temperature. This approximates a T^3 dependence. The normal operating point is at 4.8°K. If the field were zero, the temperature would have to be driven up to $T_c \sim 10.7$°K before the normal transition occurs. However, an accelerator magnet operates at nearly 90 percent of j_c at peak excitation. Since $j_c = j_o (1 - T/T_c)$, it follows that $\delta T + 0.6$°K will cause a quench to start. This corresponds to a change of enthalpy per cm of cable ~ 60 mj!

There is about 5-10 percent open space in a cable which is filled with liquid He. The helium is under some additional pressure to keep it from forming bubbles that would inhibit heat transfer from the conductor. The specific heat of liquid helium is $\sim$ 5 j/gm/°K, and there is about 10^{-3} gms of liquid/cm of cable. The effect of this added heat capacity is shown in the figure. For very short times (less than 100 sec), very high heat conduction has been observed at liquid He to metal interfaces of $\sim$ 10

$W/cm^2/^oC$. This decreases to $\sim$ 0.2 watts/$cm^2/^oK$ in the steady state. Since there is a strand surface area of about 5 cm^2/cm in a 23 conductor cable, it is apparent that the helium is well coupled to the conductor. If the helium vaporizes, the latent heat is available, and this appears as a vertical jump in heat capacity. It is difficult to transfer this quantity of heat except over long periods of time, and it probably plays no role in stabilizing the conductor.

We now examine the heat sources. They are: (a) Eddy current heating, (b) magnetization losses, (c) heating from beam losses, (d) friction from wire motion under $j \times B$ forces, and (e) microscopic fracture of the support matrix.

The first two correspond to part of the load on the central refrigerator and hence determine how rapidly the magnet can be cycled. Beam losses present a special problem. As we will see in Section 6.3, there is always enough energy in the beam of the accelerator so that if it is deposited in critical spots it will raise the temperature of the conductor sufficiently so that it will subsequently destroy itself by means of Joule heating before the current can be reduced to zero. As a consequence, the protection of the magnet from this scenario involves early detection of beam instability and aborting the beam before it gets out of control and hits the magnets. This can be done in a single turn which is a time short compared to how long it takes for

any magnetic field to change enough to cause the beam to leave the aperture, even under fault conditions.

The frictional heating of the wire is controlled by having a very solidly constrained coil package. If the wire must move, then low friction "slip planes" can be intentionally inserted in the structure.

Microscopic cracking of the support matrix is controlled by having sufficient preload so that the winding is always under compression. A very important discovery has been that epoxy must never be allowed in direct contact with the superconductor. Apparently thermal stress and mechanical stresses always cause some fracture at the interface of these materials with a resultant quench of the conductor. The elastic energy density in the coil matrix which is $1/2\ P^2/E$, is also shown in Fig.11. It is seen that the strain energy per unit volume is many times the energy necessary to quench the conductor. Of course, only a very small fraction of this energy is available from micro failures in the matrix, and even that is isolated from the conductor by the Kapton wrapping as indicated in the section on conductor.

6.2 Training

We now come to the subject of "training"(19). When a magnet is constructed and first cooled down, it has large elastic and thermal stress within the winding. As the magnet is excited, the J x B forces come into play and if

motion occurs within the winding, heat will be generated, and the magnet may quench before the critical current density is reached in the conductor. The second time the excitation is applied, a somewhat higher current may be reached before quenching until finally the full design current is achieved. This process is referred to as "training". A well constructed magnet may show very little of this phenomena, i.e. one or two quenches to full field, whereas a poorly constructed magnet may take hundreds of quenches. An extreme example of a magnet that had epoxy in direct contact with the superconductor is shown in Fig. 12.

Fig 12

6.3 Quench Heating

When a quench starts for whatever reasons at a particular point in the coil, the wire develops a finite resistance, and the temperature begins to rise. Since a certain percentage of the conductor cross section is usually made of high purity copper, the resistance is initially low, but rises steadily as the temperature increases. At the same time, the quench spreads from the point of origin with a certain velocity and new regions of conductor go normal and begin heating and developing greater resistivity. This rising resistivity coming from both the increase in temperature and the increase total length involved opposes the initial current, and if no active quench protection system is used, it is this resistance which eventually stops the current and terminates further heating.

The temperature (T) reached at any particular region of the coil can be expressed as a function of the integral of the current density squared with respect to time ($f(t) = \int i^2 dt$). This quantity f(t) can be easily obtained experimentally providing the time when the quench occurred is known. A relationship between the temperature (T) and f(T) is obtained by assuming that all the heat produced remains in the conductor, i.e. no cooling from the helium. this is a conservative assumption. We can then write:

$$i^2 \rho(T)/\alpha \, dt = C_p(T) \, dt$$

$$f(T) = \int_o^t i^2 dt = \int_{T_o}^{T} \alpha \frac{C_p(T)}{\rho(T)} dT$$

where $C_p(T)$ is the volumetric specific heat of the copper plus superconductor, $\rho(T)$ is the electrical resistivity of the copper, i the current density in the copper, and α is the fraction of the cross section that is copper. Fig. 13a shows a plot of this relationship for a particular niobium titanium conductor (Tevatron/CBA type).

The dotted line in the figure shows an approximation to this relationship(20) which assumes that the resistivity is linearly related with temperature, and the specfic heat rises as the square root of temperature, i.e.:

$$C_p = C_o\ (T/T_o)^{\frac{1}{2}}$$

$$\rho = \rho_o\ (T/T_o)$$

$$f(T) = f_o \alpha (T/T_o)^{\frac{1}{2}} \text{ where } f_o = 2C_oT_o/\rho_o$$

where C_o and ρ_o are the total mean volume specific heat and copper resistivity each at room temperature T_o. Fig. 13b and 13c show the observed and approximated dependence on temperature. This approximation while being very crude allows an analytic solution to the rise in resistivity as a function of time and gives a qualitative feel for the effect.

The volume integral of resistivity is obtained by integrating over elements of conductor volume that quenched at different times t' after the initial quench, these elements being at progressively larger distances from the point of quench origin, the distances being both along the conductor and transverse within the conductor layer.

$$\int \rho' \, dV = \frac{4w}{\alpha^3 f_o^2}\ \rho_o \frac{i^4 v_a v_\ell}{} \int_o^t t'(t-t')^2 \, dt'$$

$$= \frac{w\rho_o}{3\,\alpha^3 f_o^2}\, i^4\, v_a v_\ell\, t^4$$

where ρ' is the total resistivity of the copper and superconductor. In this approximate form the current i is

assumed to be constant with time. v_ℓ and v_a are the quench propagation velocities in the longitudinal and azimuthal directions respectively; w is the conductor width.

If the total stored energy is E, then the time (τ) before this energy has been dissipated by the resistance is given by

$$\tau = \left\{ \frac{15\ E\ f_o^2\ \alpha^3}{w\rho_o\ i^6\ v_\ell\ v_a} \right\}^{1/5}$$

In reality, of course, the current would not be constant up to this time; nevertheless, the equation gives a good approximation to the time when the current has fallen to half its value, and it allows a calculation of the maximum temperature reached (T_{max}).

$$T_{max} = T_o \left\{ \frac{15\ E\ i^4}{w\rho_o\ v_\ell\ v_a\ f_o^3\ \alpha^2} \right\}^{2/5}$$

Ignoring cooling effects, the velocity of quench propagation is given by

$$v_{\ell,a} = \frac{i}{C_p} \left\{ \frac{\rho\ k_{\ell,a}\beta}{\alpha\ (i_q - i)} \right\}^{\frac{1}{2}}$$

where i_q is the quench current density and β is the

dependence of quench current with temperature (di_q/dT). For the longitudinal case, k_ℓ is the thermal conductivity of the wire along its length, and in this case we note that ρk_ℓ is, from the Vedaman Franz Lorentz law, approximately a constant $\rho k_\ell \approx K$. The longitudinal quench velocity is thus independent of the resistivity of the wire. In the transverse direction, however, k_a is the mean thermal conductivity in the azimuthal direction which is dominated by the insulating layers between turns. For this case the velocity increases as the root of the electrical resistance of the wire.

For the purposes of quench velocity, we will take the copper resistance to be ρ_o/R where R is the resistance ratio i.e. $\rho = \rho_o/(R\alpha)$. Changes in R do not have a very significant effect on f(T) but do influence this velocity. The stored magnet energy we take to be given by:

$$E = \frac{1}{2\mu_o} \left(\frac{B}{i_q}\right)^2 r^2 \ell i^2$$

where B_q and i_q are the quench field and current densities respectively, μ_o is the vacuum magnetic permeability, ℓ is the magnet length, and r an effective high field aperture. Substituting we obtain

$$T = A \left\{ \frac{B_q^2 r^2 \ell R^{.5} i^4 (i_q - i)}{\alpha^{1.5} k_a^{.5} i_q^2 w \beta} \right\}^{.4}$$

where

$$A = T_o \left\{ \frac{7.5\, C_p^{\,2}}{\rho_o^{\,1.5}\, f_o^{\,3}\, K^{.5}\, \mu_o} \right\}^{.4}$$

We see that the maximum temperature is encountered when the current is at 4/5 of the quench current and that this maximum temperature is then

$$T \propto \left\{ \frac{B_q^{\,2}\, r^2\, \ell\, R^{.5}\, i_q^{\,3}}{\alpha^{1.5}\, k_a^{\,.5}\, w\, \beta} \right\}^{.4}$$

Since $B \propto i\, w\, n$ and $i_{cu} = i/\alpha$ (where n is the number of layers), we can finally write:

$$T \propto \left\{ \frac{B^{3.5}\, r^2\, \ell\, R^{.5}\, i_{cu}^{\,1.5}}{n^{1.5}\, w^{2.5}\, k_a^{\,.5}} \right\}$$

from which it is easy to calculate the allowable copper current density for a given magnet. We note that allowable current density falls with increasing field, aperture, and magnet length. Somewhat surprisingly it rises when a lower copper resistance ratio R is used, this being due to the increased transverse quench propagation in this case.

Experimental measurements have been made on the damage thresholds both for the electrical insulation and for the superconducting properties of the wire. No electrical

degradation was observed even with values of the $\int i^2 dt$ as high as 9.7 10^7 amps^2 mm^{-4} seconds. Whereas slight reduction of the superconducting properties of niobium titantium cable were observed at approximately 8.4 10^8 amps^2 mm^{-4} seconds. Both values correspond to extremely high temperatures (above 1000°K). In an experiment on an actual magnet connected in series to other magnets with no protection provided, no damage was observed with an $\int i^2 dt$ = 9.58 10^8 amps^2 mm^{-4} seconds, but substantial damage was done at a value of 10. Again we note that these numbers correspond to extremely high temperatures, and we must remember that the calculations assume negligible cooling either by conduction or by gas convection during the quench process. In the case of the actual magnet test, it is clear that some cooling must be present.

6.4 Quench Protection

The simplest form of protection is to provide no protection at all and have the resistance in the magnets absorb all available energy. But if no protection of any kind is provided, a magnet will be required to absorb the energy of an entire string of magnets assuming that these are connected in series. Something has to be done.

The easiest protection scheme is to place a high current solid state diode across each magnet with a direction such as to allow the main current to bypass the magnet in the forward direction through the diode, see

Fig. 13d. If a typical solid state diode is operated at near $4^{o}K$ then it is found that a relatively large forward voltage (of the order of 4 volts) is required before conduction begins. Providing the excitation rate does not require a voltage across the magnet greater than about 4 volts, the diode will not conduct unless a quench occurs. When the magnet quenches, however, a large voltage is induced, the diode becomes conducting and the main current can pass through the diode instead of through that magnet. As a result, the magnet is only required to absorb its own quench energy and not that of other magnets in the string. The requirements for this have been described above but may in some cases result in very high temperatures being reached. These are somewhat reduced if the upper and lower coil halves each have a separate diode (as was done in CBA (Fig. 13e). The simplicity and reliability of this protection scheme are its greatest attractions.

An alternative protection scheme used in the Tevatron(21) involves sensing the presence of a quench electronically and then putting a pulse of current into an electrical heater causing a more generally distributed quench in the magnet or magnets of a string. When this is done, the maximum temperature in the magnets can be kept to a relatively low value, considerably lower than in the diode scheme. The disadvantage of such an active system is that a failure in the system could cause the loss of magnet and

great care has to be exercised in the detailed design. It is not clear whether or not such an active system can be extrapolated to a system as extended as the SSC. However, quench protection will be a dominant consideration for large accelerators using high field (> 4 T) magnets.

References

1. Boom, R. W., McIntyre, P., Mills, F. E., 1983 Workshop on Technical Discussions on the SSC Magnets, Argonne, informal report

2. Wilson, R. R., 1982 Proc. DPF Summer Study on Elementary Particle Physics and Future Facilities, Snowmass, pp. 330-34

3. Allinger, J. A., Danby, G. T., Jackson, J. W., Prodell, A., 1977 High Precision Superconducting Magnets, IEEE Trans. Nucl. Sci., NS-24:1299

4. Lundy, R. A., 1981 IEEE Trans. on Magnetics, Vol. MAG-17, No. 1:709-12

5a. Palmer, R. B., Cottingham, J. G., Fernow, R. C., Goodzeit, C. L., Kelly, E. R., et al. 1981. BNL Internal Report, TLM No. 23, BNL, Upton, NY

5b. Palmer, R. B., Baggett, N. V., Dahl, P. F. 1983. IEEE Trans. Magnetics, Knoxville, MAG-19, No. 3, Part I, pp. 189-94

6a. Palmer, R. B. 1982. BNL (CBA) Tech Note 427, BNL, Upton, NY

6b. CBA Newsletter No. 2. 1982. 2-in-1 Magnet, p. 27, BNL, Upton, NY

7. Biallas, G., Finks, J. E., Strauss, B. P., Kuchnir, M., Hanson, W. B., et al. 1979. IEEE Trans. on Magnetics, Vol. MAG-15, No. 1:131-3

8. Cooper, W. E., Fisk, H. E., Gross, D. A., Lundy, R. A., Schmidt, E. E., et al. 1983. IEEE Trans. on Magnetics, Vol. MAG-19, No. 3

9. Larbalestier, D. C. 1983. Part. Accel Conf., IEEE Trans. on Nucl. Sci., 1983 (in press)

10. Tollestrup, A. V. 1979. IEEE Trans. on Magnetics, Vol. MAG-15, No. 1:647-53

11. Althaus, R., Caspi, S., Gilbert, W. S., Hassenzahl, W., Mauser, R. et al. 1981. IEEE Trans. on Nucl. Sci., Vol. NS-28, No. 3:3280-82

12. Kahn, S. A., Engelmann, R., Fernow, R. C., Greene, A. F., Herrera, J. C. 1983. Proc. Part. Accel. Conf., Santa Fe (in press)

13a. Hanft, R., Brown, B. C., Cooper, W. E., Gross, D. A., Michelotti, L., et al. 1983. IEEE Trans. in Nucl. Sci., 1983 Accel. Conf., Santa Fe (in press)

13b. Schmidt, E. E., Brown, B. C., Cooper, W. E., Fisk, H. E., Gross, D. A., et al. 1983. IEEE Trans. in Nucl. Sci., 1983 Accel. Conf., Santa Fe (in press)

14. Blesser, E. J., Thompson, P. A., Wanderer, P., Willen, E. 1983. DPF Workshop, Ann Arbor (in press)

15. Tannenbaum, M. J., Ghosh, A. K., Robins, K. E., Sampson, W. B. 1983. Proc. Part. Accel. Conf., Santa Fe (in press)

16a. Ciazynski, D., Mantsch, P. 1981. IEEE Trans. on Nucl. Sci., Vol. NS-28, No. 3:3280-82

16b. Ciazynski, D., Mantsch, P. 1981. IEEE Trans. on magnetics, Vol. MAG-17, No. 1:165-7

17. Tollestrup, A. V., Peters, R. E., Koepke, K., Flora, R. H. 1977. IEEE Trans. on Nucl. Sci., Vol. NS-124, No. 3:1331-33

18. Koepke, K., Kalbfleisch, G., Hanson, W., Tollestrup, A. V., O'Meara, J., et al. 1979. IEEE Trans. on Magnetics, Vol. MAG-15, No. 1:658-61

19. Tollestrup, A. V. 1981. IEEE Trans. on Magnetics, Vol. MAG-17, No. 1:863-72

20. Wilson, M. N. 1983. Superconducting Magnets. Clarendon Press. Note that although this reference uses this approximation, the following treatment is not equivalent, but follows that by Alan Stevens, private communication

21. Koepke, K., Rode, C., Tool, G., Flora, R., Jostlein, H., et al. 1981. IEEE Trans. on magnetics, Vol. MAG-17, No. 1:713-15

TABLE I

	Calculated $\times 10^4$	Observed $\times 10^4$	Ratio	Corresponding Displacement Error μ
b_0		6.10		
b_2	2.1	1.76	.84	55
b_4	1.0	.73	.73	48
b_6	.5	.24	.48	32
b_1	3.8	.84	.22	15
b_3	1.3	.24	.18	12
b_5	.7	.35	.5	33
a_2	2.1	.45	.21	14
a_4	1.0	.19	.19	13
a_6	.5	.10	.20	13
a_1	3.8	2.44	.64	42
a_3	1.3	.73	.56	37
a_5	.7	.37	.53	35

TABLE II

		Effect from 1 mrad (66μ)			Error from Table I	
Type of Error	Term	Inside Layer $\times 10^{-4}$	Outside Layer $\times 10^{-4}$	Total Effect $\times 10^{-4}$	Obs.	RMS μ
a) Both poles to right	Δb_1	2.6	1.5	4.1	.84	14
b) Both midplanes up	Δa_1	2.2	1.7	4.0	2.4	40
c) One midplane up, other down	Δa_2	.8	1.1	1.8	.45	16
d) Coil non-uniformity	Δb_2	2.6	.9	3.5	1.8	34
e) Radius of all coils	Δb_0	6.8	2.1	8.9	6.1	45

Figure Captions

Figure 1 Magnet types: (a) Warm iron superferric, (b) cold iron superferric, (c) high field picture frame, (d) cold iron cosine theta, (e) warm iron cosine theta, and (f) two-in-one cosine theta. Where, 1: beam pipe, 2: conductor, 3: iron yoke, 4: cryostat, 5: hole to correct saturation.

Figure 2 Approximations to cosine theta coil: (a) Pure cosine theta, (b) intersecting ellipse, (c) two layer approximation, (d) two layer with wedges, (e) rectangular block

Figure 3 Cryogenic systems: (a) Force flow, (b) two phase jacket, (c) force flow with separate two phase exchanger. Where 1: magnet, 2: high pressure single phase, 3: two phase, 4: J.C. valve, 5: low pressure gas.

Figure 4 B-J-T surface for NbTi.

Figure 5. (a) B-J curves for NbTi at $4.2^{\circ}K$ and $1.8^{\circ}K$. The lower curve is a typical guaranteed minimum from an industrial source. The upper curve is what may be achieved optimally(9). (b) Comparison of NbTi at $1.8^{\circ}K$ with Nb_3Sn at $4.2^{\circ}K$. See reference(9).

Figure 6 Shielding currents and field in a slab of superconductor exposed to increasing (a) and decreasing fields (b) according to the Bean model.

Figure 7 Photomicrograph of the end of a strand of a superconductor cable. The copper matrix has been etched back to expose the NbTi filaments which are about 8 μ across.

Figure 8 End sextupole effect. (a) 0-z plot of normal coil end, section xx shows central cross section, section yy shows end cross section with blocks moved towards poles creating sextupoles, (b) end with wedge to remove effect.

Figure 9 Field dependent effects. (a) Sextupole in non-saturating iron magnet showing persistent current effect, (b) as above with saturation effects also, (c) saturation effect on transfer function.

Figure 10 Force per linear inch of conductor in the Tevatron two-shell magnet at 4 T.

Figure 11 This diagram shows the various energies contained in a volume equal to that of 1 cm of cable in a Tevatron dipole at 4 T. The operating point is at $4.6^{\circ}K$, and the short sample limit would be reached at $5.6^{\circ}K$.

Figure 12 Example of a magnet with extremely bad training. A well-built magnet will show no changes after the first or second quench.

Figure 13 Quench protection. (a), (b), and (c) show functions of temperature with solid lines showing measured values and dashed showing simple approximations: (a) integral i^2dt, (b) electrical resistivity of copper, (c) specific heat of copper, (d) and (e) show single and double diode protection circuits.

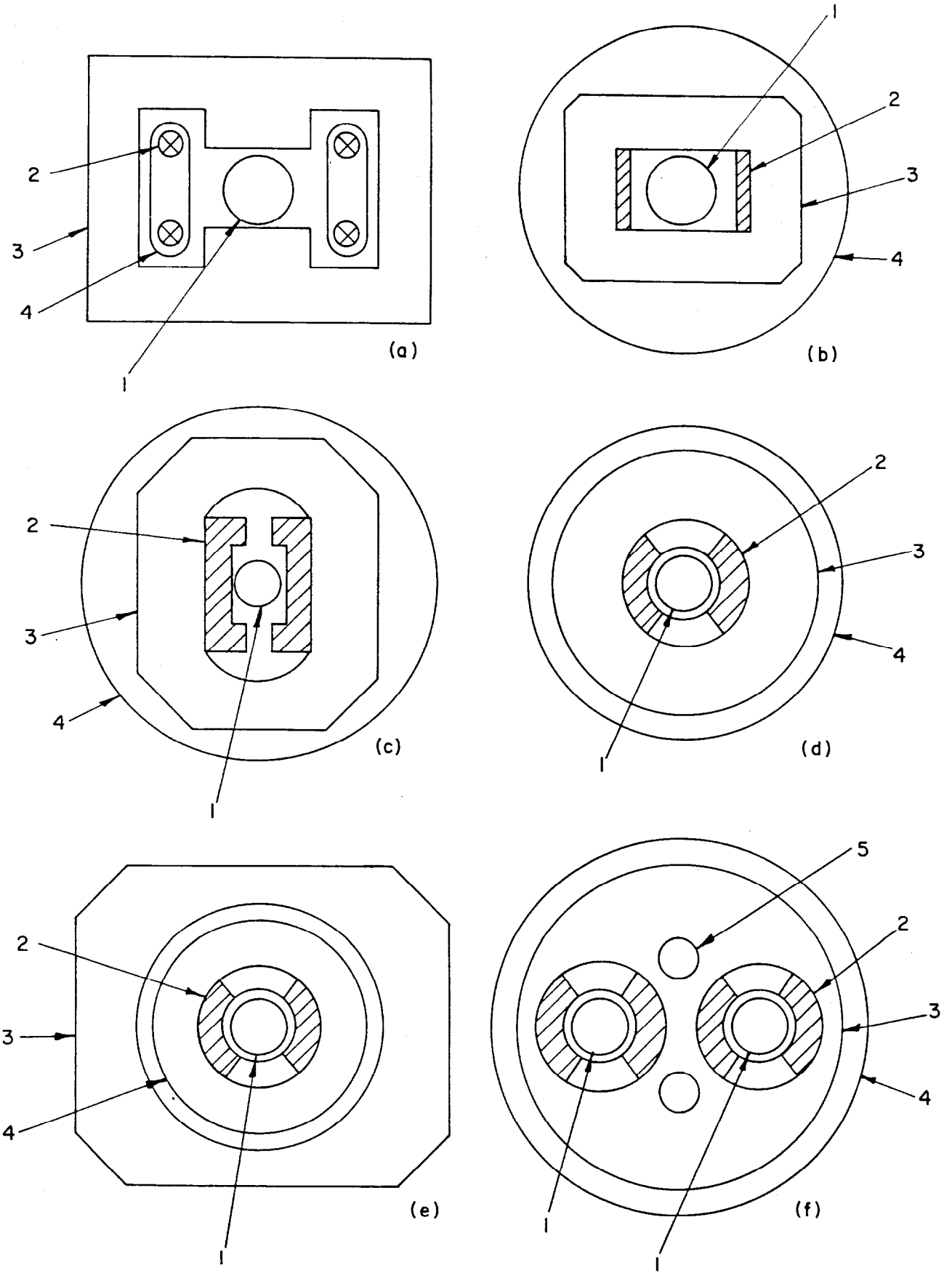

Figure 1

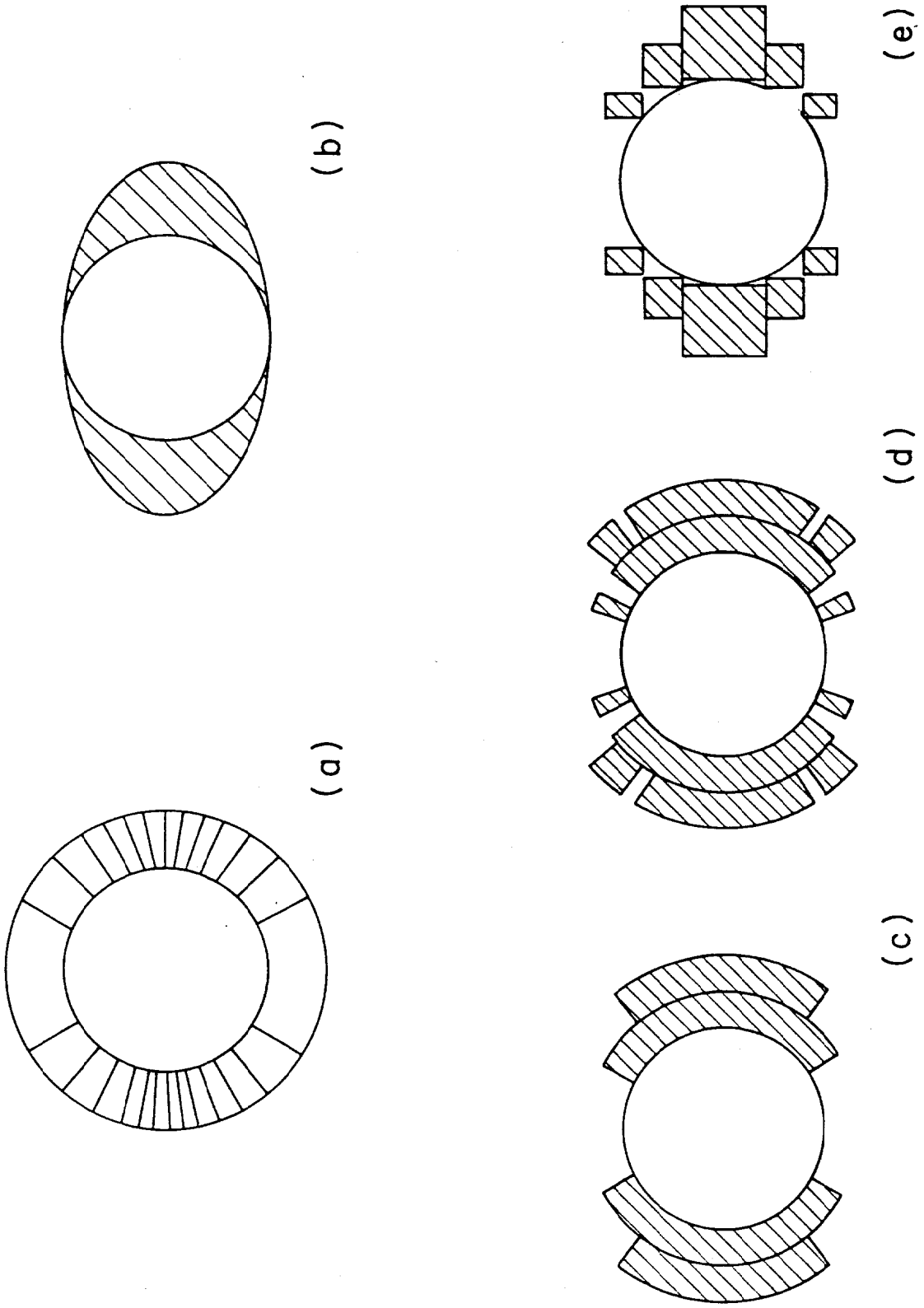

Figure 2

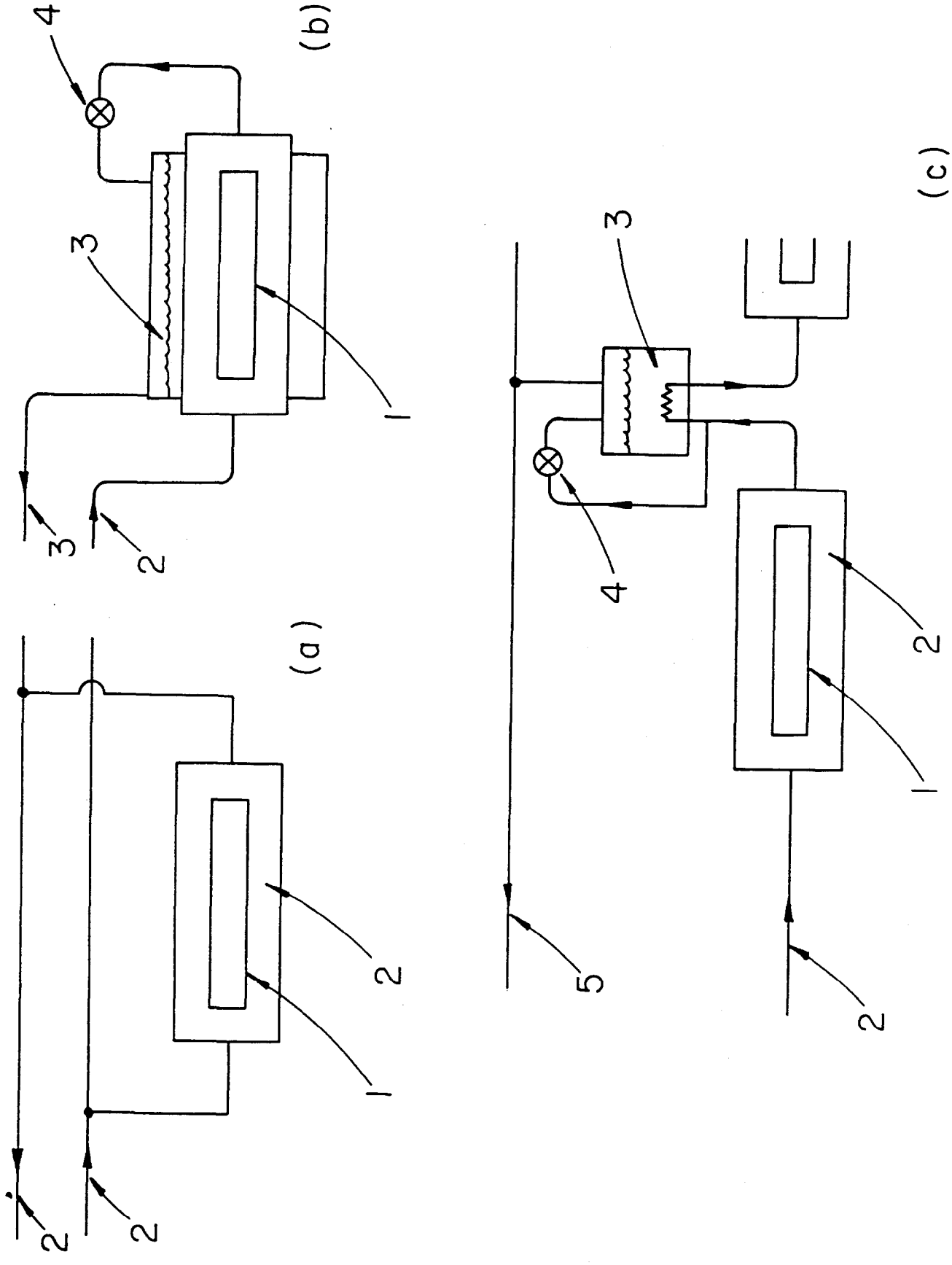

Figure 3

CRITICAL SURFACE

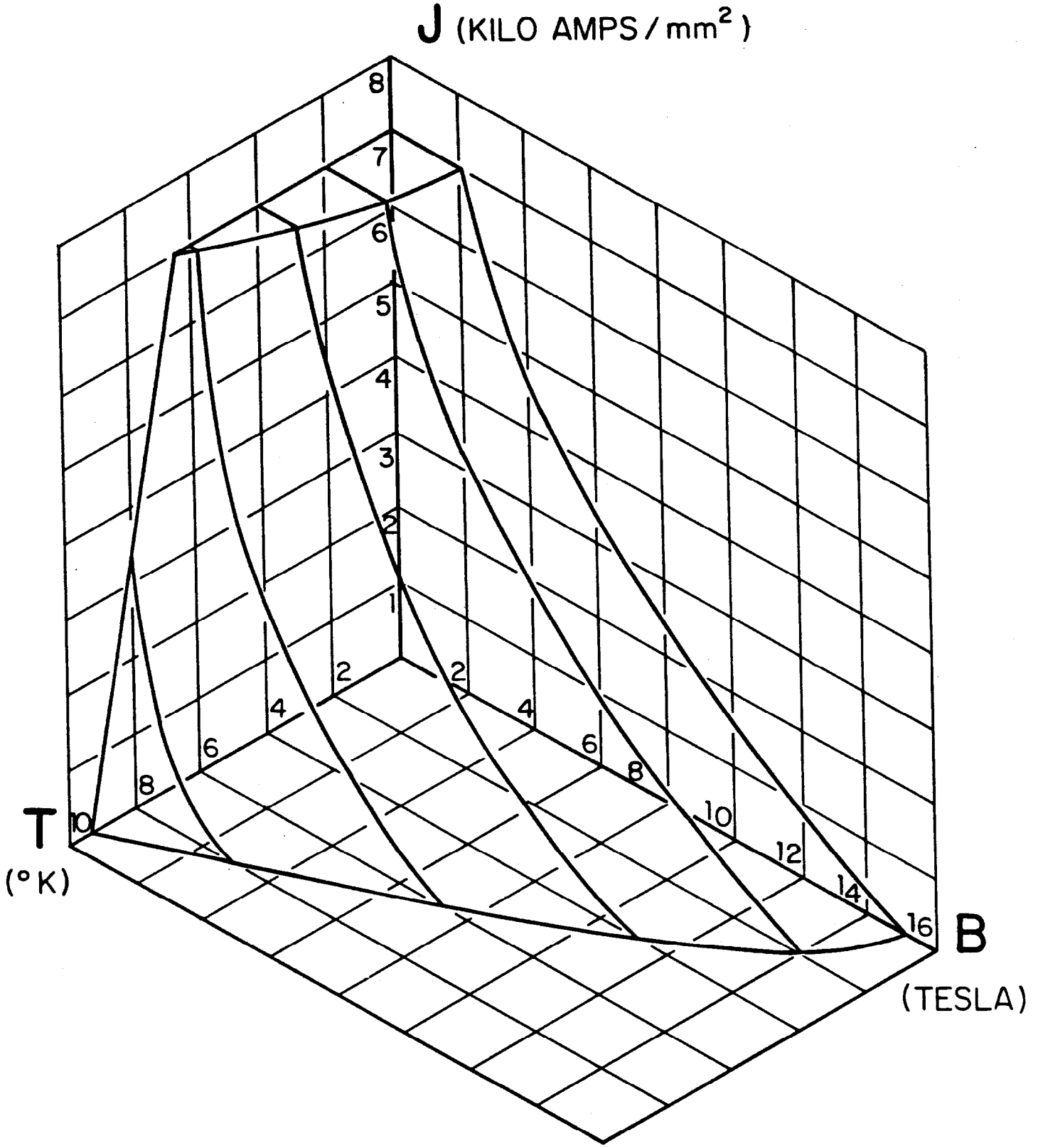

Figure 4

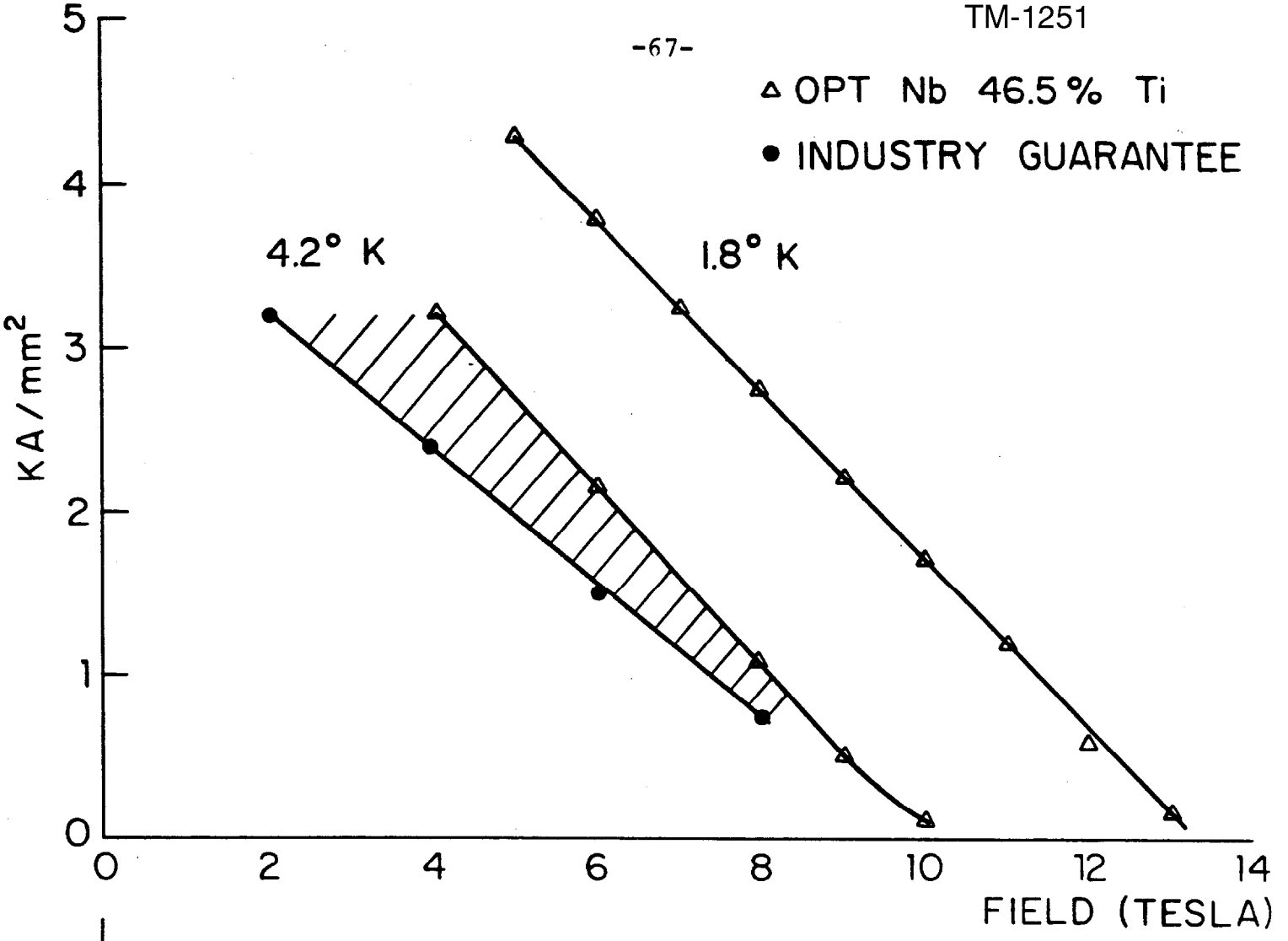
△ OPT Nb 46.5% Ti
● INDUSTRY GUARANTEE
4.2° K
1.8° K
KA/mm²
FIELD (TESLA)

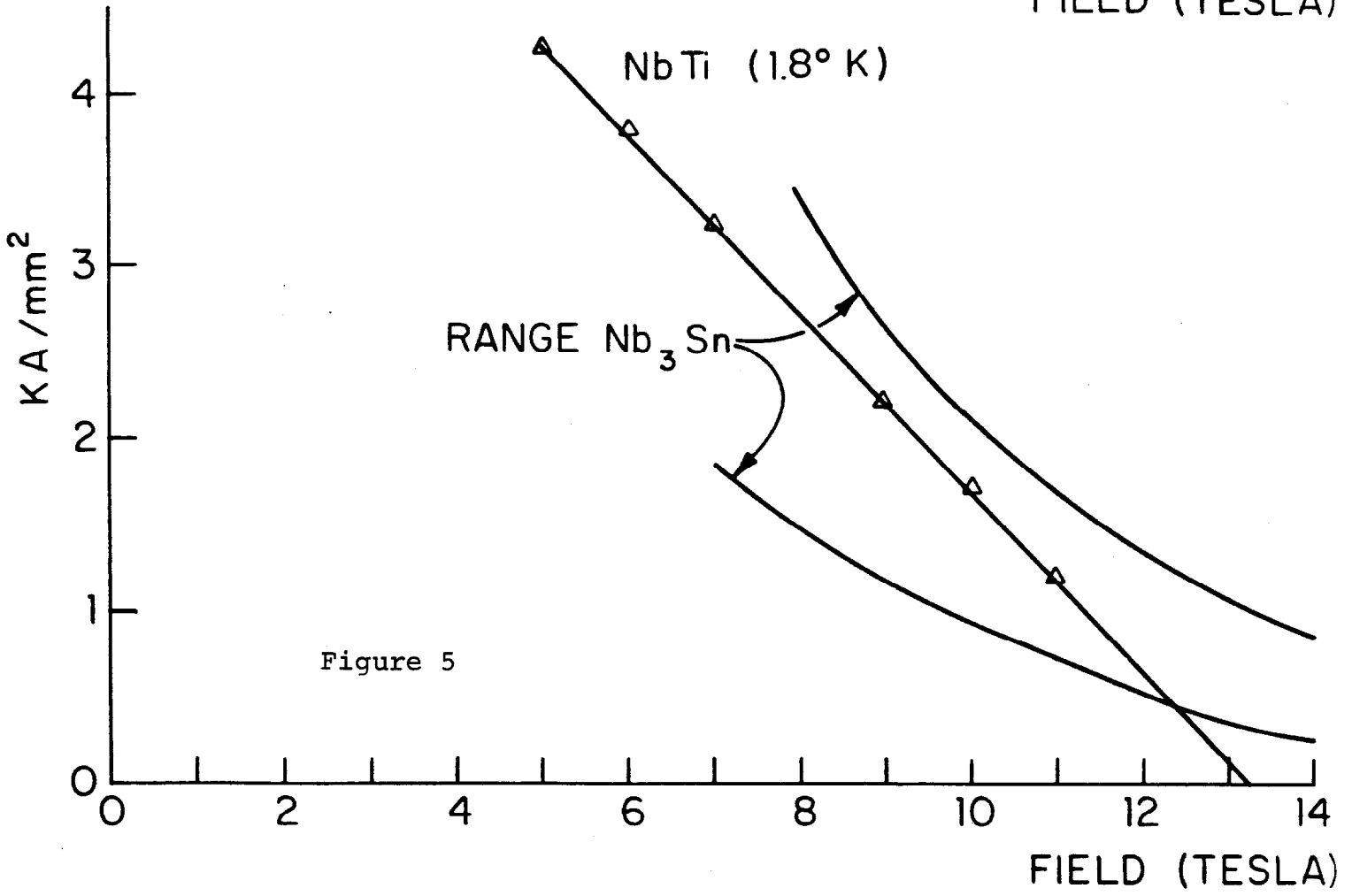
NbTi (1.8° K)
RANGE Nb3Sn
KA/mm²
FIELD (TESLA)

Figure 5

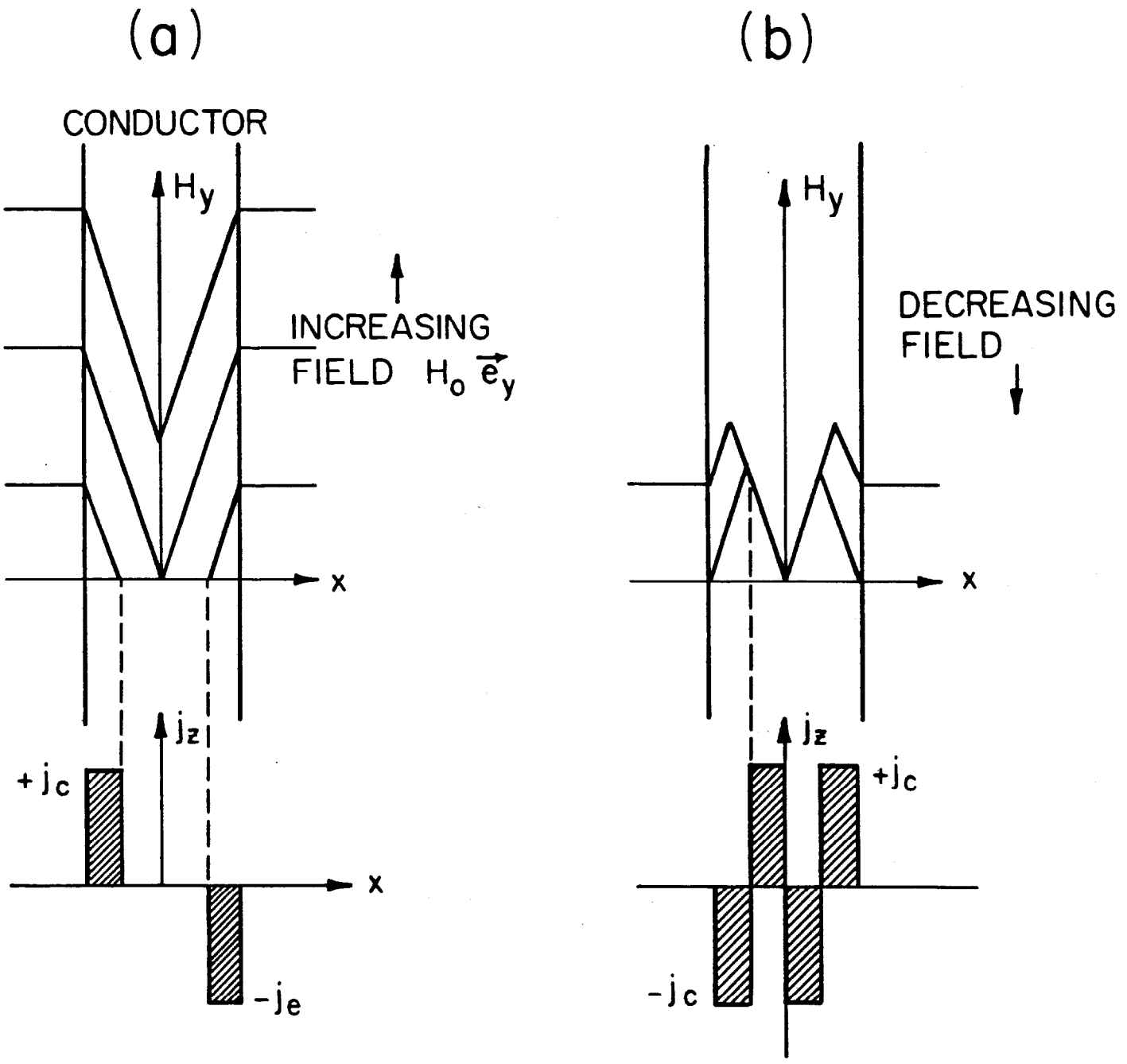
(a)
CONDUCTOR
H_y
INCREASING
FIELD $H_o \vec{e}_y$
x
j_z
$+j_c$
x
$-j_e$
(b)
H_y
DECREASING
FIELD
x
j_z
$+j_c$
$-j_c$

Figure 6

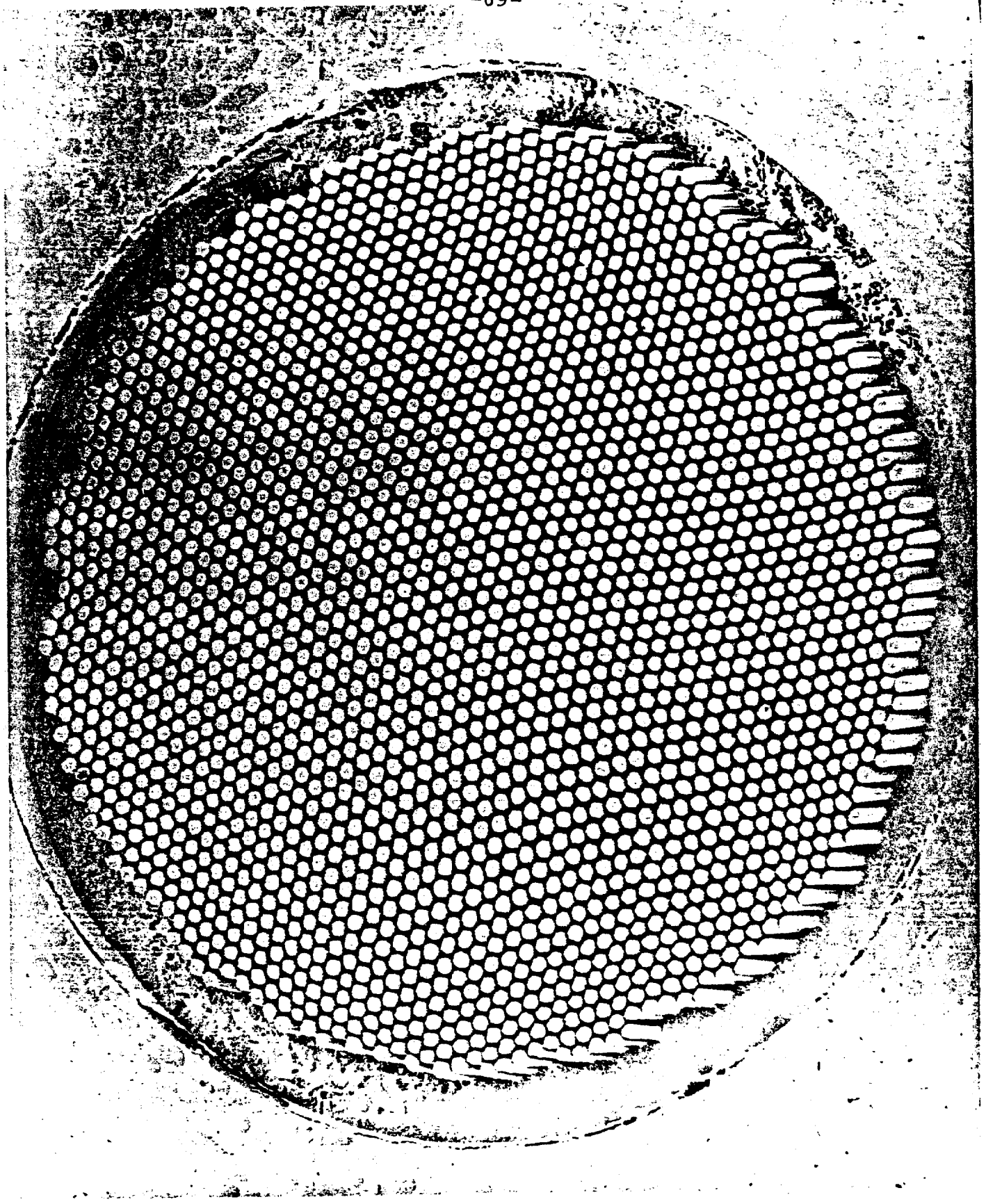

Figure 7

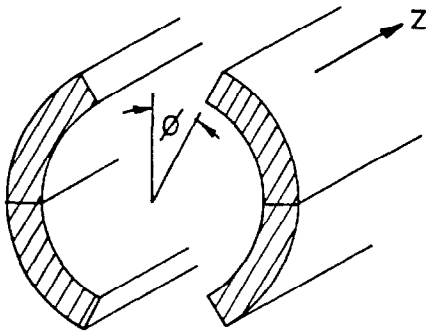

SECTION XX

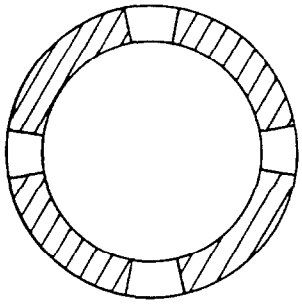

SECTION YY

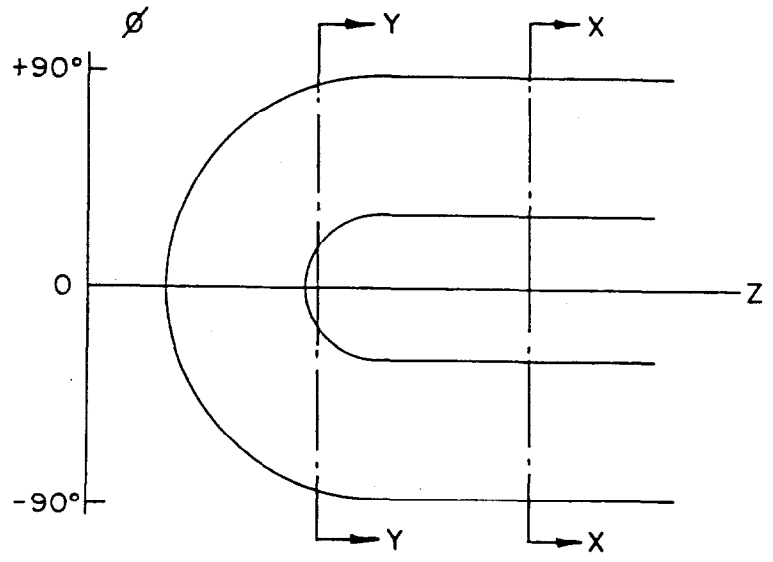

(a)

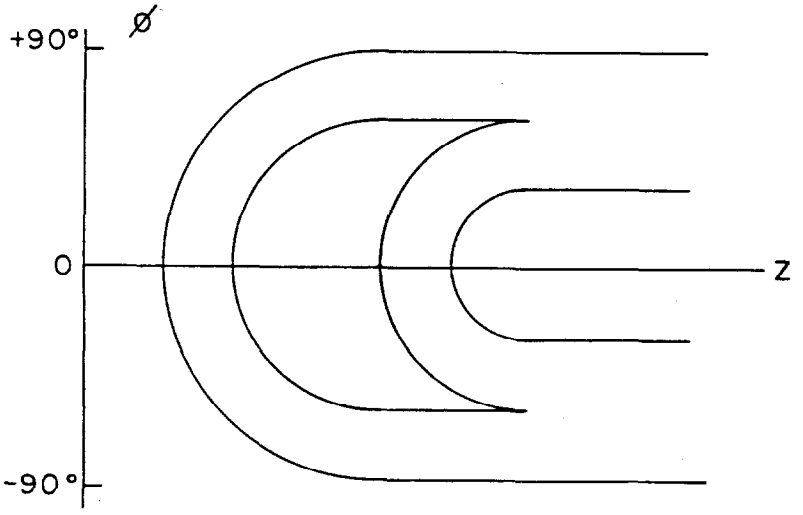

(b)

Figure 8

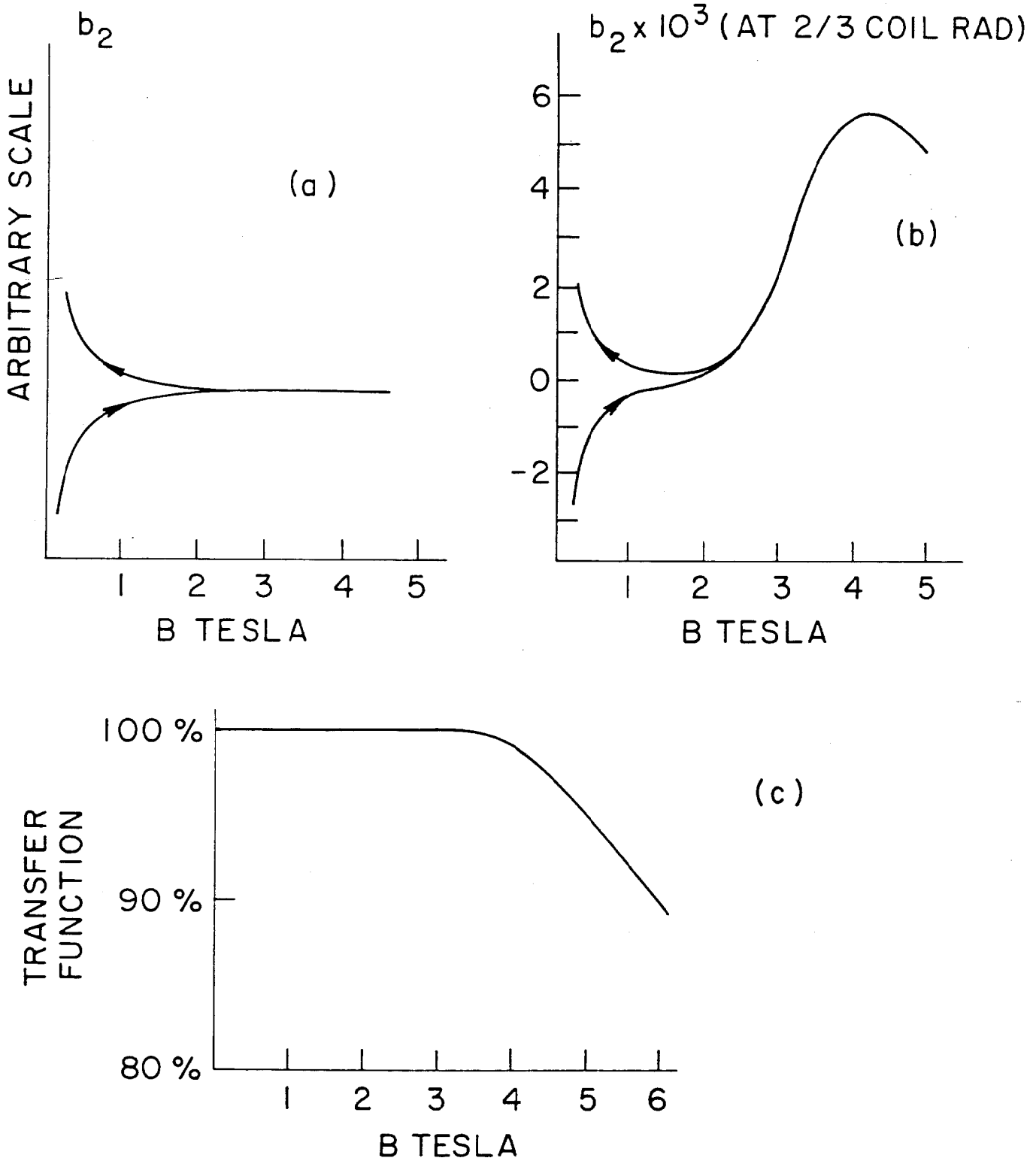
b_2
ARBITRARY SCALE
(a)
1 2 3 4 5
B TESLA
$b_2 \times 10^3$ (AT 2/3 COIL RAD)
6
4
2
0
-2
(b)
1 2 3 4 5
B TESLA
100 %
90 %
80 %
TRANSFER FUNCTION
(c)
1 2 3 4 5 6
B TESLA

Figure 9

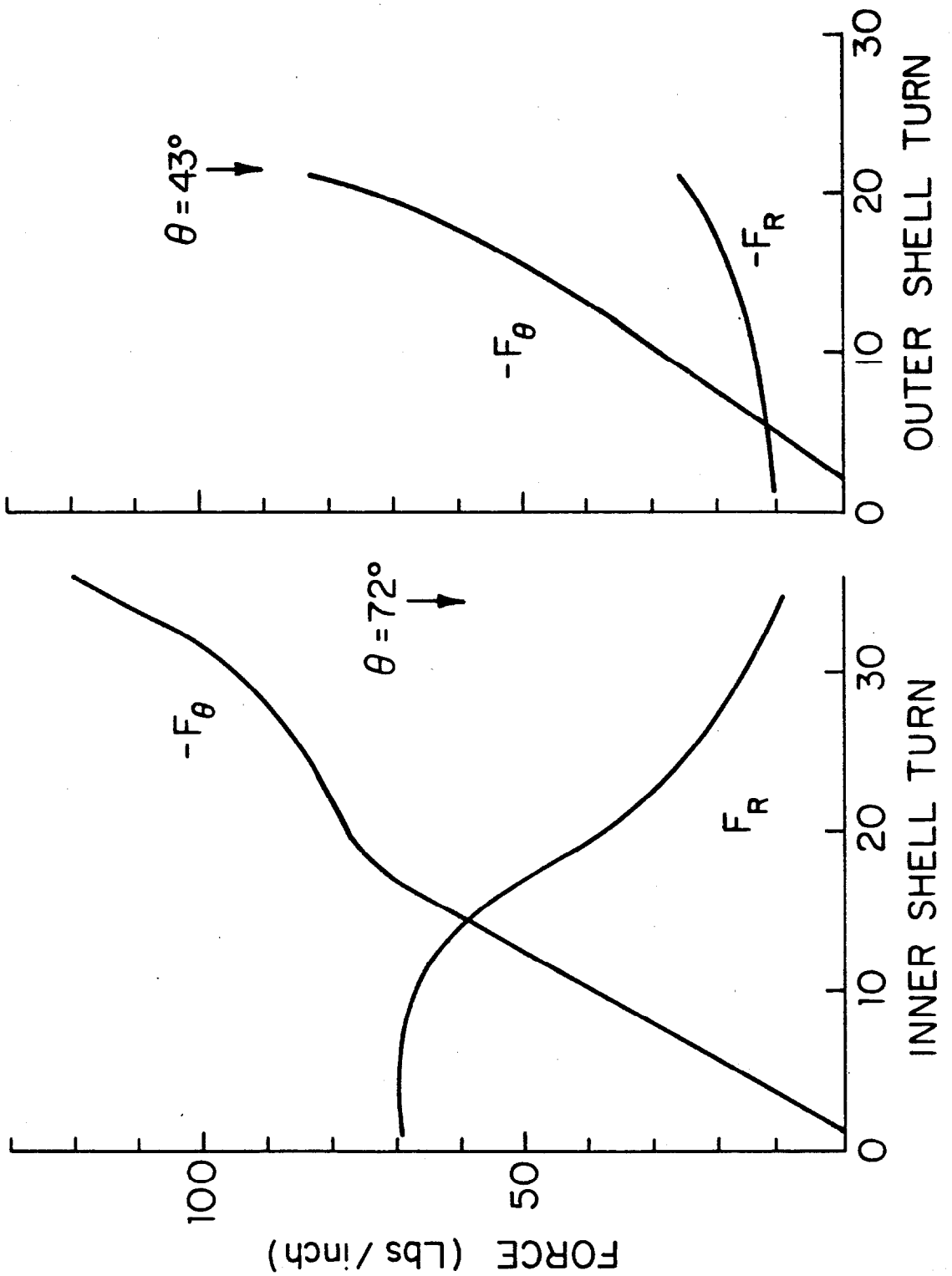
FORCE (Lbs / inch)
100
50
0
10
20
30
INNER SHELL TURN
$-F_\theta$
F_R
$\theta = 72°$
$\theta = 43°$
$-F_\theta$
$-F_R$
0
10
20
30
OUTER SHELL TURN

Figure 10

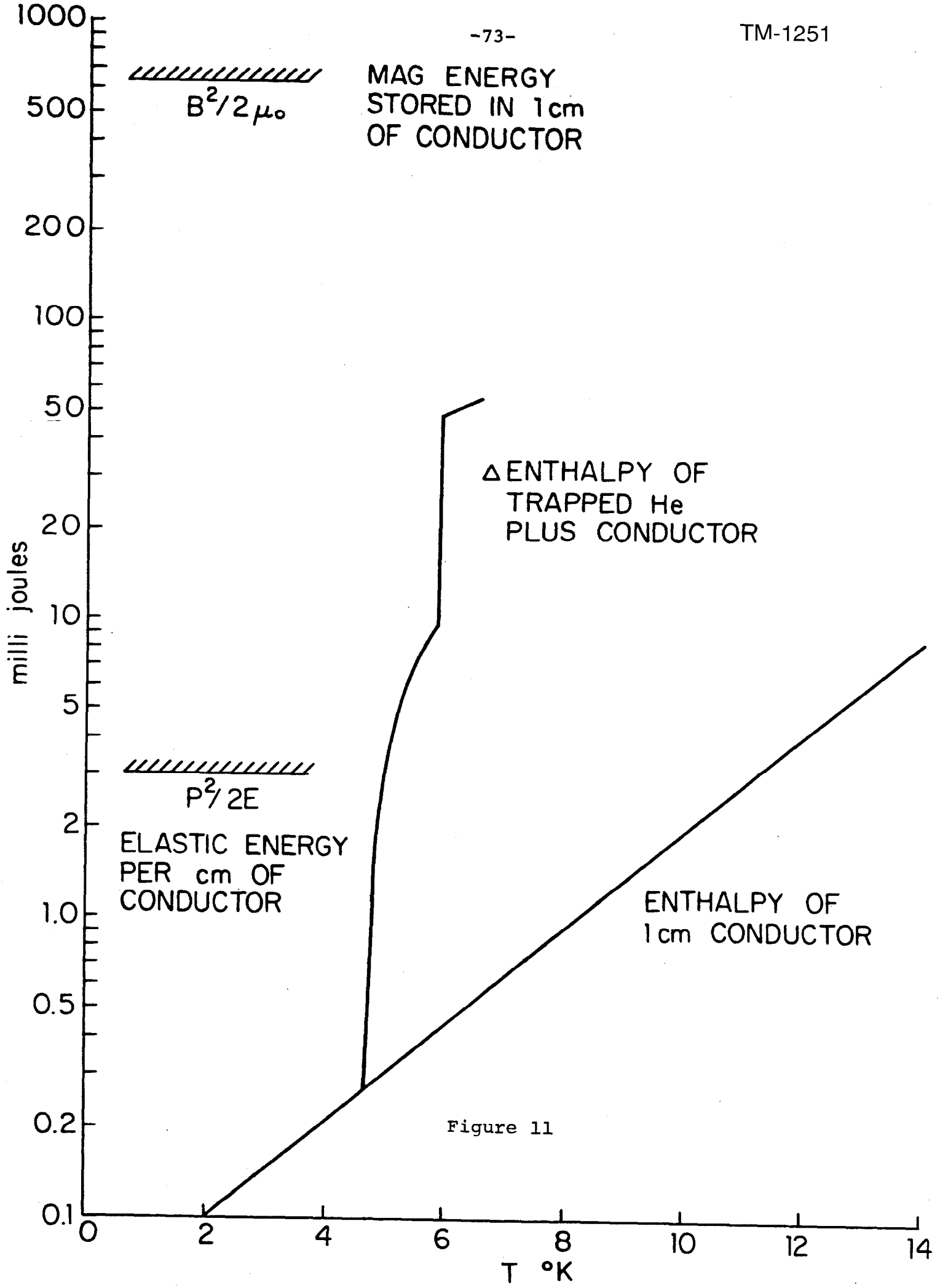
1000
500
200
100
50
20
10
5
2
1.0
0.5
0.2
0.1
milli joules
$B^2/2\mu_o$
MAG ENERGY STORED IN 1cm OF CONDUCTOR
ΔENTHALPY OF TRAPPED He PLUS CONDUCTOR
$P^2/2E$
ELASTIC ENERGY PER cm OF CONDUCTOR
ENTHALPY OF 1cm CONDUCTOR
0
2
4
6
8
10
12
14
T °K

Figure 11

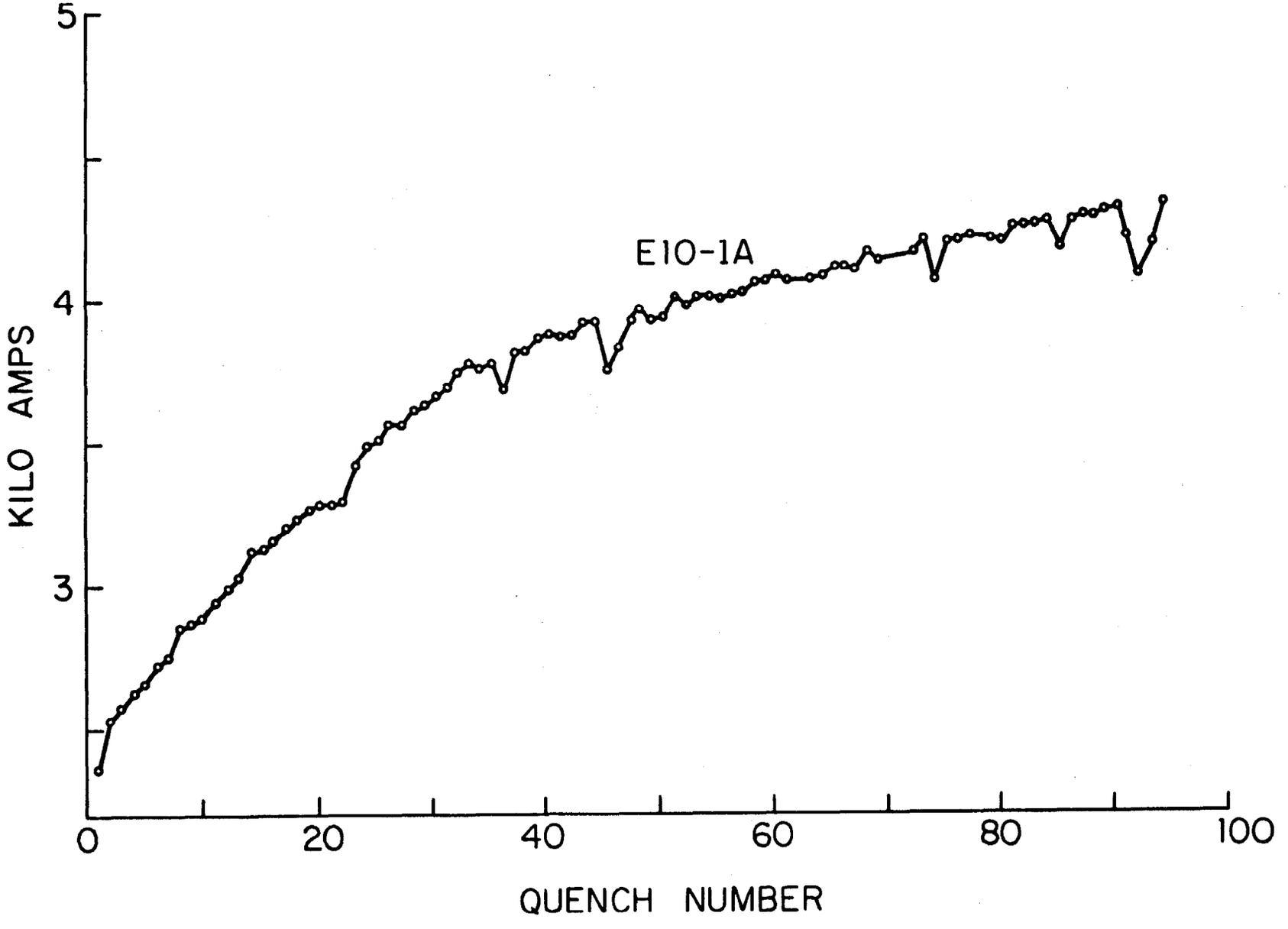

Figure 12

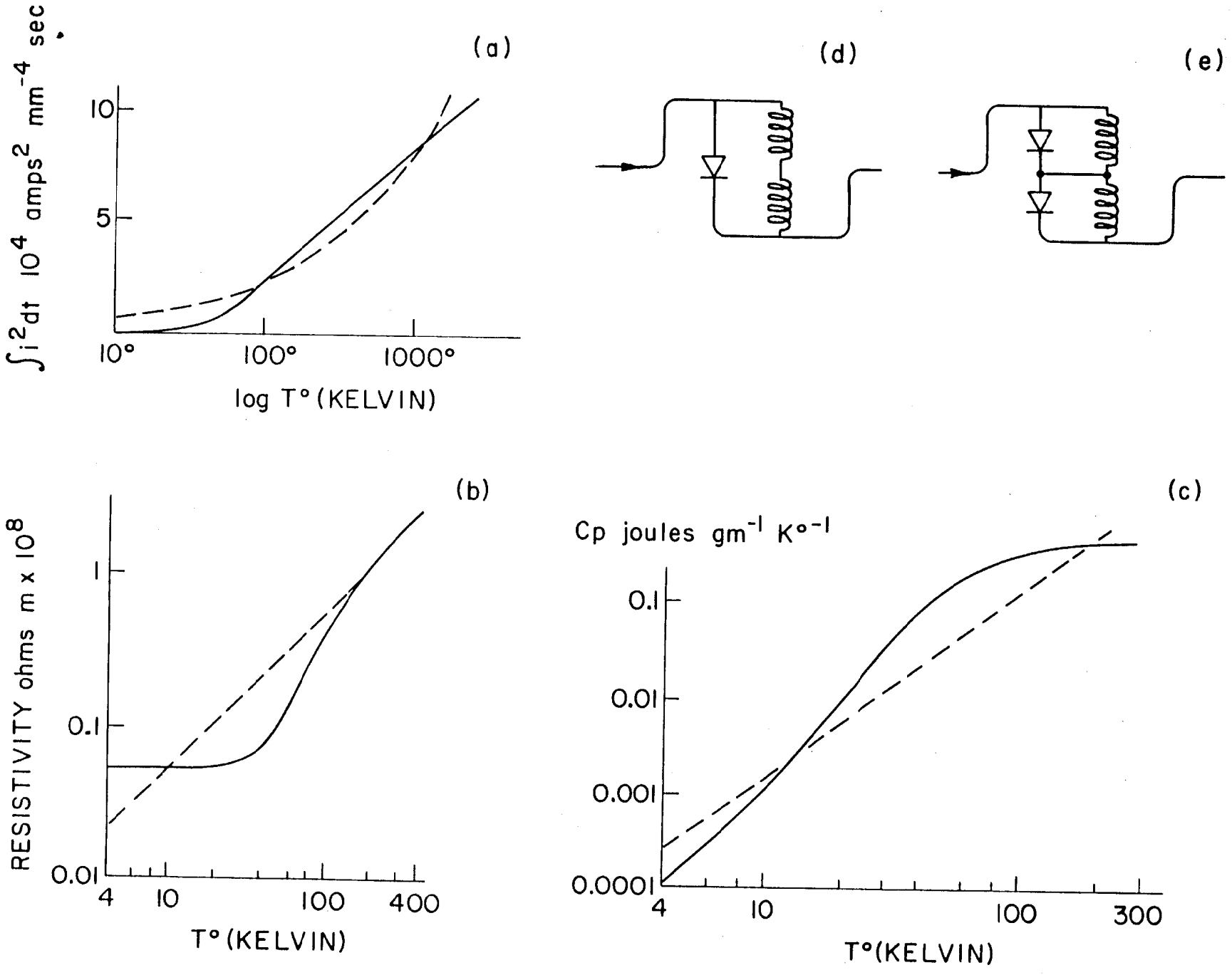
(a)
$\int i^2 dt \; 10^4$ amps^2 mm^{-4} sec
10
5
10°
100°
1000°
log T° (KELVIN)
(d)
(e)
(b)
RESISTIVITY ohms m x 10^8
1
0.1
0.01
4
10
100
400
T° (KELVIN)
(c)
Cp joules gm^{-1} K°$^{-1}$
0.1
0.01
0.001
0.0001
4
10
100
300
T°(KELVIN)

Figure 13